THE CHEMOKINE RECEPTOR CXCR7 FUNCTIONS IN ENDOCARDIAL-DERIVED CELLS TO REGULATE CARDIAC VALVE REMODELING

APPROVED BY SUPERVISORY COMMITTEE

Michelle D. Tallquist, Ph.D.

Steven A. Kliewer, Ph.D.

Helen L. Yin, Ph.D.

Deepak Srivastava, M.D.

DEDICATION

To my parents and wife, Hyojung,

for their unconditional love.

THE CHEMOKINE RECEPTOR CXCR7 FUNCTIONS IN ENDOCARDIAL-DERIVED CELLS TO REGULATE CARDIAC VALVE REMODELING

by

SANGHO YU

DISSERTATION

Presented to the Faculty of the Graduate School of Biomedical Sciences

The University of Texas Southwestern Medical Center at Dallas

In Partial Fulfillment of the Requirements

For the Degree of

DOCTOR OF PHILOSOPHY

The University of Texas Southwestern Medical Center at Dallas

Dallas, Texas

December, 2009

ACKNOWLEDGEMENTS

I could not have finished my graduate work without help from many people throughout my school years both in science and life. First of all, I am truly indebted to my mentor, Dr. Deepak Srivastava, for his guidance and care in every aspects of my time in his lab. Especially when I had difficult times, his sincere concern and advice helped me overcome those tough times.

I am grateful to my dissertation committee members, Drs. Michelle Tallquist, Steven Kliewer, and Helen Yin, for sound advice and support. I am exceptionally thankful for their understanding my situation of working off-campus in San Francisco, CA, and allowing me to have my defense seminar without the final committee meeting.

I want to thank many former and current members of the Srivastava lab for their support and discussions. Especially I want to thank those I have worked closely with and have spent more time with: Jason Fish, Takatoshi Tsuchihashi, Alecia Muth, Kim Cordes, Masaki Ieda, Joseph Shieh, Li Qian, and Chong Park. I also wish to thank colleagues in other labs or institutions for help from providing reagents to scientific discussions: Timothy Behrens, Dianna Crawford, Peter Chang, Thomas Schall, Guy Cinamon, and Jason Long.

I cannot overemphasize how crucial emotional support and encouragement from my friends have been during my graduate years. I want to thank Euiseok Kim, Misung Kim, Wonsuk Chung, Hakkyun Kim, Weon-Kyu You, Sangwon Suh, Jason Fish, and Kim Cordes.

I would like to express my gratitude to my parents and parents-in-law for their care, support, and love. Most importantly, I would love to thank my wife Hyojung. She has loved me, understood me, supported me, and cheered me. Without her unconditional love, I would not have overcome ordeals during my thesis work. She is my lover and best friend.

THE CHEMOKINE RECEPTOR CXCR7 FUNCTIONS IN ENDOCARDIAL-DERIVED CELLS TO REGULATE CARDIAC VALVE REMODELING

SANGHO YU, Ph.D.

The University of Texas Southwestern Medical Center at Dallas, 2009

DEEPAK SRIVASTAVA, M.D.

Cardiac disease is the number one killer in developed countries and congenital heart diseases are the most common birth defects worldwide. The heart supplies nutrients and oxygen to the entire body, therefore the proper development and function of the heart is essential for survival of an organism. During looping and maturation phases of heart development, proper separation of the outflow tract and chambers, and correct connection to the existing vascular system are critical to ensure unidirectional blood flow and supply of oxygenated blood to the rest of the body. Cardiac neural crest cells and endocardial cushions contribute significantly to these remodeling processes.

Cardiac valves are fibrous tissues that separate atria from ventricles and ventricles from great vessels, and allow unidirectional blood flow through the heart. They are derived from specific sets of endocardial cells in the outflow tract and atrioventricular canal. Cardiac valvulogenesis is a highly ordered process and small perturbations in any of signaling pathways involved can result in fatal consequences. As a result, cardiac valve anomaly is one of the most common congenital heart diseases.

CXCR7 is a chemokine receptor whose function in the heart is unknown. Unexpected cardiac phenotypes of *Cxcr7* knockout mice prompted further investigation to elucidate its role during heart development. I speculated that CXCR7 functions during cardiac valve formation due to its high expression in cushion endocardial and mesenchymal cells, and the phenotype of *Cxcr7* knockout mice at birth: cyanotic pups and enlarged hearts. Histological analysis of *Cxcr7* knockout hearts at different developmental stages revealed that the aortic and pulmonary valves were thickened during late valve remodeling. This was due to unchecked proliferation of cushion mesenchymal cells as revealed by phospho-histone H3 staining. Increased proliferation was due to increased BMP signaling in the cardiac cushions even though direct interaction between CXCR7 and BMP signaling is unclear. Endothelial cell-specific deletion of *Cxcr7* using *Tie2-Cre* resulted in hypertrophy of the heart in adult mice because of semilunar valve stenosis, confirming important function of CXCR7 in endocardial-derived cells. This study provides valuable insight into the mechanism controlling cardiac cushion mesenchymal cell proliferation and may contribute to better diagnosis, treatment, and prevention of cardiac valve defects in humans.

TABLE OF CONTENTS

PRIOR PUBLICATIONS

Kwon, H.J., Lee, K.W., **Yu, S.**, Han, J.H., and Kim, D.S. (2003). NF-kappaB-dependent regulation of tumor necrosis factor-alpha gene expression by CpG-oligodeoxynucleotides. Biochem Biophys Res Commun *311*, 129-138.

Srivastava, D., and **Yu, S.** (2006). Stretching to meet needs: integrin-linked kinase and the cardiac pump. Genes Dev *20*, 2327-2331.

Saxena, A., Fish, J.E., White, M.D., **Yu, S.**, Smyth, J.W., Shaw, R.M., DiMaio, J.M., and Srivastava, D. (2008). Stromal cell-derived factor-1alpha is cardioprotective after myocardial infarction. Circulation *117*, 2224-2231.

Fish, J.E., Santoro, M.M., Morton, S.U., **Yu, S.**, Yeh, R.F., Wythe, J.D., Ivey, K.N., Bruneau, B.G., Stainier, D.Y., and Srivastava, D. (2008). miR-126 regulates angiogenic signaling and vascular integrity. Dev Cell *15*, 272-284.

Yu, S., Crawford, D., Tsuchihashi, T., Behrens, T.W., Srivastava, D. The chemokine receptor CXCR7 functions in endocardial-derived cells to regulate cardiac valve remodeling. *In preparation.*

LIST OF FIGURES

CHAPTER ONE

CHAPTER TWO

CHAPTER THREE

CHAPTER FOUR

LIST OF TABLES

LIST OF APPENDICES

LIST OF ABBREVIATIONS

APC	adenomatous polyposis coli
ASD	atrial septal defect
AVC	atrioventricular canal
BMP	bone morphogenetic protein
CHD	congenital heart disease
CRABP1	cellular retinoic acid binding protein 1
CXCR7	CXC chemokine receptor 7
DIG	digoxigenin
ECC	endocardial cushion
ECM	extracellular matrix
EGF	epidermal growth factor
EMT	endothelial-to-mesenchymal transformation
ERK	extracellular signal-activated kinase
FGF	fibroblast growth factor
FHF	first heart field
FOXH1	forkhead box h1
GAG	glycosaminoglycan
GATA	GATA-binding protein
GPCR	G protein-coupled receptor
HA	hyaluronic acid
HAND1/2	heart and neural crest derivatives expressed transcript 1/2

HAS2	hyaluronan synthase 2
HB-EGF	heparin-binding epidermal growth factor
HIV	human immunodeficiency virus
ISL1	Islet1
LACZ	β-galactosidase
LVEDD	left ventricular end diastolic dimension
LVESD	left ventricular end systolic dimension
MAPK	mitogen-activated protein kinase
MEF2C	myocyte enhancer factor 2c
NCC	neural crest cell
NFATc1	nuclear factor of activated T cells cytoplasmic 1
NKX2-5	NK2 transcription factor related, locus 5
OFT	outflow tract
PCR	polymerase chain reaction
pH3	phospho-histone H3
PI3K	phosphoinositide 3 kinase
PKB	protein kinase B
pSmad1/5/8	phospho-Smad1/5/8
RBP-Jκ	recombination signal-binding protein for immunoglobulin κJ region
RT	room temperature
SDF1	stromal cell-derived factor 1
SHF	second heart field
Shh	sonic hedgehog

SL	semilunar
SNP	single nucleotide polymorphism
TF	transcription factor
TGF	transforming growth factor
TK	thymidine kinase
TUNEL	terminal deoxynucleotidyl transferase-mediated dUTP nick end labeling
VEGF	vascular endothelial growth factor
VIP	vasoactive intestinal peptide
VSD	ventricular septal defect

CHAPTER ONE

INTRODUCTION

Cardiac Morphogenesis

Congenital heart disease (CHD) is the most common birth defect which affects 1-2% of newborns worldwide and is the leading cause of death in infants under 1 year of age [1, 2]. Additionally, heart disease is the number one mortality factor in adults in the United States and 5 million suffer from various kinds of cardiac insufficiencies [3]. Increasing numbers of genes involved in cardiac morphogenesis and their associations with CHD are being elucidated, but their exact mechanisms of action are largely unknown. However, evidence from human familial and large scale single nucleotide polymorphism (SNP) studies of cardiac patients has revealed that many genes involved in early cardiac development also play critical roles in the adult heart [4]. It is thus crucial to understand the mechanisms underlying cardiac morphogenesis for better prevention, diagnosis, and treatment of not only CHD but cardiac disease in general.

In vertebrates, the heart is the first organ to form and is highly susceptible to perturbations during development mainly due to the complexity of cardiogenesis. Despite differences in cardiac structures in different species, from a simple pumping tube of insects to the complex four-chambered machinery of mammals, the overall mechanism of cardiogenesis is highly evolutionarily conserved. Decades of studies in various model organisms have helped us better understand the overall process of cardiac morphogenesis and the regulation of cardiac gene expression, and new factors are being added to an already complicated network of transcription factors (TFs) and signaling molecules

involved in cardiogenesis (reviewed in [1, 5]). However, more detailed cellular and molecular mechanisms of these genes are relatively less known. Such knowledge will require further investigations about the target genes of cardiac TFs and signaling molecules.

Cardiac Precursors and Chamber Formation

Recent studies have revealed that there are two sources of cardiac progenitor cells, the first heart field (FHF) and second heart field (SHF), instead of a single source of these cells as previously believed [6]. Cells in the FHF derive from the anterior lateral plate mesoderm and form a cardiac crescent around embryonic day (E) 7.5 in mouse embryos (Fig.1A). These cells migrate to the ventral midline and fuse to form an early heart tube composed of myocardial and endocardial cells separated by extracellular matrix (ECM), also known as cardiac jelly. At the same time, SHF cells also migrate to the midline and position themselves dorsal to the FHF in the pharyngeal mesoderm [1] (Fig. 1B). The heart tube then undergoes rightward looping, during which the posterior region moves anteriorly, followed by an expansion of myocardium that leads to the formation of recognizable cardiac chambers [6] (Fig.1C). Right after cardiac tube formation, SHF cells are recruited to the poles of the cardiac tube, and the progenitor cells added to the venous pole contribute to the formation of the inflow region and atria, while cells added to the arterial pole give rise to the outflow tract (OFT) and right ventricle myocardium [7-11]. The early heart tube composed of FHF cells basically has a left ventricular identity [10]. LIM homeodomain transcription factor *Isl1(Islet1)* serves as a marker for the SHF. Results from lineage tracing of *Isl1*-expressing cells and *Isl1* knockout mice further

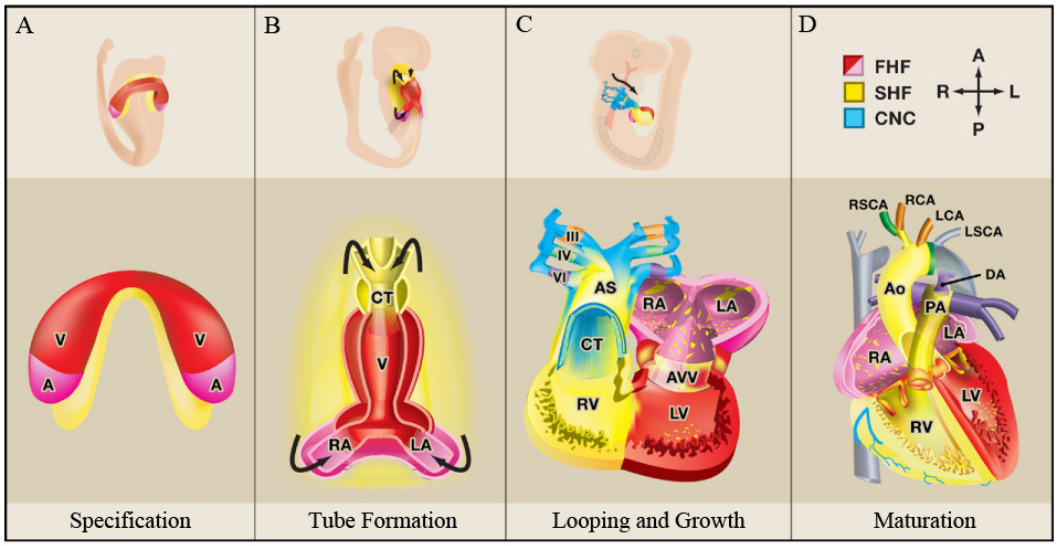

Figure 1. Mammalian Cardiac Morphogenesis. Oblique views of whole embryos and frontal views of cardiac precursors during mammalian cardiac development are shown. **A.** The first heart field (FHF) cells form a crescent shape in the anterior embryo (red and pink) while the second heart field (SHF) cells position themselves medial and dorsal to the FHF (yellow). **B.** FHF cells migrate to the midline and fuse to form a linear heart tube with SHF cells later migrating into the anterior and posterior poles to form the right ventricle (RV), conotruncus (CT), and part of the atria. **C.** After the looping of the heart, cardiac neural crest cells (NCCs) migrate into the outflow tract and contribute to the septation of great vessels and morphogenesis of aortic arch arteries (blue). **D.** Further remodeling process results in the four-chambered heart. V, ventricle; LV, left ventricle; LA left atrium; RA, right atrium; AS, aortic sac; Ao, aorta; PA, pulmonary artery; RSCA, right subclavian artery; LSCA, left subclavian artery; RCA, right carotid artery; LCA, left carotid artery; DA, ductus arteriosus. (Modified from [1]).

corroborated the previous findings that the heart forms from two different sources of cardiac progenitor cells [11]. Also, a retrospective analysis using β-galactosidase labeling in mouse embryos showed that the FHF contributes to both ventricles, atrioventricular canal (AVC), and both atria, whereas the SHF contributes to the OFT, right ventricle, and both atria [12].

Cardiac looping morphogenesis is the earliest manifestation of left-right asymmetries in the developing organism. Expansion of myocardium during a looping process occurs through differential proliferation at the outer curvature of the cardiac tube [13, 14]. In addition, intracardiac flow forces have been shown to play a role during cardiac growth [15]. The most highly proliferative cardiomyocytes are located along the

outer layer of the heart, a region referred to as the compact zone [16]. Signals from the overlying epicardium are necessary and sufficient to promote proliferation of cardiomyocytes within the compact zone. One example is retinoic acid produced by the epicardium. Deletion of retinoic acid receptor *Rxr*α in mice causes defective myocardial expansion, resulting in thin-walled ventricles [17, 18]. Signals from the endocardium are also important for cardiac chamber growth. Neuregulin growth factors are secreted from the endocardium and their myocardial receptor ErbB2 and ErbB4 are required for myocardial growth since knockout mice of *EbrB2*, *ErbB4*, or *neuregulin-1* develop cardiac growth defects characterized by the absence of trabeculae, the finger-like projections of ventricular cardiomyocytes [19-21]. Much less is known about the growth of atria. The orphan nuclear receptor COUP-TFII is required for atrial, but not ventricular growth [22].

The looped heart undergoes an extensive remodeling process, as well as myocardial growth, including septation of the ventricles and atria, cardiac valve formation, development of a conduction system, and patterning of the OFT and proximal great vessels (Fig.1D). Mechanisms controlling these remodeling processes are relatively less known except for the case of valve formation, which will be discussed in a separate section. A subset of ventricular cardiomyocytes differentiates into Purkinje cells that form the cardiac conduction system. Endothelin-1 secreted from coronary arteries regulates this process [23]. Septation and patterning of the OFT require the function of neural crest cells (NCCs). Cardiac NCCs are derived from the otic primordia to the third somite, and migrate through the pharyngeal arches to the OFT of the heart. Mutations affecting their migration or differentiation cause OFT and aortic arch anomalies

(reviewed in [24]). Interactions between cardiac NCCs and SHF cells seem to be paramount for proper OFT morphogenesis [1].

Transcriptional Regulation of Cardiac Morphogenesis

Early cardiac specification of progenitor cells at the anterior lateral plate mesoderm is an interplay between both positive and negative signals from neighboring tissues, especially the endoderm and neural tube (reviewed in [25]). These signaling pathways include bone morphogenetic protein (BMP), sonic hedgehog (Shh), fibroblast growth factor (FGF), Wnt, and Notch pathways. In response to these signals, early cardiac TFs begin to be expressed in cardiac progenitor cells, such as *Nkx2-5* (NK2 transcription factor related, locus 5), *Gata4* (GATA-binding protein 4), *Isl1*, *Mef2c* (myocyte enhancer factor 2c), and T-box transcription factors [26]. These TFs cooperatively regulate expression of downstream cardiac genes and modulate various aspects of cardiac morphogenesis. Mutations of multiple genes that encode for various proteins, from TFs to structural proteins, have been associated with human syndromes with cardiac defects or isolated cardiac abnormalities, and most of the same gene mutations in model organisms successfully recapitulated these phenotypes. Conversely, mutations causing cardiac defects in the model organisms have led to the discoveries of causative gene mutations in human conditions. From studies of cardiac gene mutations, it is obvious that no single factor is essential for cardiac development [6]. Loss of one cardiac factor seems to be partially compensated by other family members or different cardiac TFs.

Nkx2-5 mutant mice fail to proceed beyond the linear cardiac tube stage and die around E9.5 [27, 28]. These mice display severe defects in ventricular morphogenesis

and fail to express *Hand1* (heart and neural crest derivatives expressed transcript 1), a basic helix-loop-helix TF that is predominantly expressed in the left ventricle, while *Hand2*, which marks the right ventricle, is still expressed, suggesting defects in the FHF lineage [29, 30]. *Hand1* is required for left ventricular growth as loss of *Hand1* results in a hypoplastic left ventricle due to a proliferation defect [31-33]. Conversely, lack of *Hand2* in mice produces right ventricle hypoplasia [34, 35]. Interestingly, *Nkx2-5/Hand2* double mutants are completely devoid of a ventricle, which is more severe than *Hand1/Hand2* double mutant phenotype, implying *Nkx2-5* has more cardiac target genes in addition to *Hand1* [30, 32]. *Nkx2-5* mutations have been identified in families with various CHDs including ventricular septal defects (VSDs), atrial septal defects (ASDs), and conduction defects [36, 37].

The zinc-finger TF GATA4 and two related members, GATA5 and GATA6, are expressed in the precardiac mesoderm and the developing heart of different vertebrate species [38]. Studies from mouse, chick, zebrafish, and fly have shown the important function of GATA factors during cardiogenesis [39-42]. For example, cardiac progenitor cells of *Gata* mutants in mouse and chick fail to fuse at the midline (cardiac bifida) and have decreased *Nkx2-5* expression [39, 40]. In humans, mutations in *Gata4* cause ASDs and VSDs, and the disrupted interactions between GATA4 and Nkx2-5, and between GATA4 and Tbx5 possibly underlie these phenotypes [43].

T-box TFs also participate in various areas of cardiac development and their mutations are associated with cardiac defects in humans. *Tbx5* starts to be expressed in early cardiac progenitor cells but its expression becomes rapidly restricted to a posterior region of the cardiac tube, which gives rise to the left ventricle, atria, and sinus venosus

[44-46]. *Tbx5* knockout mice display left ventricular hypoplasia and sinoatrial defects but the growth of the OFT and right ventricle is unaffected, indicating that defects have a FHF origin [47]. Meanwhile, forced expression of *Tbx5* in the myocardium disrupts right ventricular growth with up-regulation of *Hand1* but down-regulation of *Hand2* [48]. These results suggest a function for *Tbx5* in left ventricular specification. Holt-Oram syndrome in humans is caused by *Tbx5* mutations and cardiac defects of these patients are similar with those of *Nkx2-5* mutations [49, 50]. Further experiments demonstrated that Tbx5 and Nkx2-5 function cooperatively through their physical interactions [47, 51]. GATA4, Tbx5, and Nkx2-5 may form a complex to regulate cardiac chamber septation.

In contrast to *Tbx5*, which functions in the FHF, *Tbx1* functions in the SHF. Knockout mice of *Tbx1* have growth and septal defects of the OFT, and aortic arch patterning defects [52-55]. The OFT septal and aortic arch defects are probably due to cardiac NCC abnormalities because *Tbx1* regulates cardiac NCC migration and differentiation in the pharyngeal arches through activation of *Fgf8* and *Fgf10* [56-60]. In 22q11 microdeletion syndrome (also known as DiGeorge syndrome), *Tbx1* is responsible for cardiac and craniofacial disorders including persistent truncus arteriosus and interrupted aortic arch [54, 55].

Another T-box TF, Tbx20, plays a role in both the FHF and SHF by regulating myocardial expansion. *Tbx20* knockout mice lack *Hand1* expression, indicating its role in the FHF, and have a hypoplastic right ventricle and disrupted OFT, implying its role in the SHF [61-64]. Tbx20 promotes myocardial growth by inhibiting *Tbx2* and *Isl1* expressions and by activating *Mef2c* and *Nkx2-5* expressions synergistically with Isl1 and GATA4 [14, 62, 65, 66].

Table 1. Mutant Phenotypes of Key Cardiac Transcription Factors

Gene	Crescent expression	Second heart field expression	Mutant phenotype	Human phenotype
Nkx2-5	Yes	Yes	Loss of ventricular tissue, no *Hand1* expression	ASD, VSD, conduction defect
Hand1	Yes	No	Hypoplastic LV	-
Hand2	Yes	Yes	Hypoplastic RV	-
Gata4	Yes	Yes	Cardiac bifida	ASD, VSD
Tbx5	Yes	No	Sinoatrial defects, hypoplastic LV	ASD, VSD, conduction defect
Tbx1	Yes	Yes	OFT defect, aortic arch defect	OFT defect
Tbx20	Yes	Yes	Chambers do not develop, no *Hand1* expression, hypoplastic RV, OFT defects	ASD, VSD
Isl1	No	Yes	Single atrium and ventricle (LV identity), OFT defect, atrial defect,	-
Mef2c	(Yes?)	Yes	OFT defect, hypoplastic RV, INF defect	-
Foxh1	No	Yes	OFT defect, hypoplastic RV	-

ASD, atrial septal defect; VSD, ventricular septal defect; LV, left ventricle; RV, right ventricle; OFT, outflow tract; INF, inflow region. (Modified from [6]).

LIM-homeodomain TF Isl1 not only marks the SHF but regulates migration, proliferation, and survival of cardiac progenitor cells [11]. *Isl1* knockout mice have only two cardiac chambers, one atrium and one ventricle, and genetic marker expressions showed that the ventricle has left ventricular identity [11]. Intriguingly, lineage tracing of *Isl1*-expressing cells revealed that these cells also populate a part of the left ventricle, probably recruited in a delayed fashion [11]. Also, rare $Isl1^{+}$ cells mark undifferentiated cardiac progenitor cells in the adult heart, making them good potential therapeutic targets for cardiac repair [67].

Other TFs involved in SHF development are Mef2c and Foxh1 (forkhead box h1). *Mef2c* mutant mice have a reduced OFT, hypoplastic right ventricle, and disrupted sinus venosus, suggesting its function in SHF cells [68]. *Foxh1* mutants have similar SHF phenotypes to *Mef2c* mutants but do not display atrial defects [69]. *Mef2c* seems to be a downstream target of Isl1, GATA4, and Foxh1/Nkx2-5, and may regulate myocardial growth [66, 69].

Recent findings suggest that key regulators of cardiac development may also have important functions in the adult heart [5]. Therefore, survivors of CHDs may be predisposed to cardiomyopathy later in life. For example, mutations of *Gata4* or *Tbx20* were identified in patients with cardiomyopathy, apart from heart structural damages during development [43, 70]. Also, ventricle-specific *Nkx2-5* deletion in mice suggested the role of this gene in the postnatal conduction system [71]. Mutant phenotypes of genes described above are summarized in Table 1.

Cardiac Valve Formation

Cardiac valves are required for unidirectional blood flow through the heart and their correct positioning is also critical for proper chamber septations. Cardiac valve malformation is the most common cardiac defect, accounting for 25% to 30% of all CHDs [72]. A number of congenital valve defects have been identified as components of human syndromes, such as Down syndrome (cardiac cushion defects), Leopard syndrome (pulmonic stenosis), 22q11 deletion syndrome (truncus arteriosus), Holt-Oram syndrome (pulmonic stenosis), Alagille syndrome (pulmonic stenosis), and Noonan syndrome (pulmonic stenosis) [73, 74]. In cases of Holt-Oram syndrome, Alagille syndrome, and

Noonan syndrome, the genetic causes were identified [47, 49, 50, 75-77]. However, in most cases, congenital cardiac valve defects occur separately from any known human syndrome or genetic cause [74].

Congenital cardiac valve defects often have mild or no phenotypes in early ages but predispose affected individuals to various cardiovascular disorders in later life, requiring valve replacement or extensive treatment [2]. Better understanding of developmental and remodeling processes of cardiac valves should benefit the advent of new therapies for valve anomalies.

Overview of Cardiac Valve Formation

The early cardiac tube consists of an outer myocardial layer and an inner endocardial layer separated by the ECM known as the cardiac jelly [74] (Fig. 2). Right after looping of the cardiac tube (around E9.5 in mouse), a subset of endothelial cells in two valve forming regions, one in the AVC and the other in the OFT, is specified by signals from underlying myocardium and delaminates and migrates into the cardiac jelly, a process referred to as endothelial-to-mesenchymal transformation (EMT) [78] (Fig.2). Migrated cells subsequently proliferate and differentiate into valve mesenchymal cells to form swellings, known as the endocardial cushions (ECCs) [79] (Fig.2).

Cells in the ECCs further differentiate and secret ECM components such as collagen, elastin, and proteoglycans to convert the ECCs into thinly tapered mature valves [80] (Fig.2). This process involves apoptosis and extensive remodeling of the ECM but the overall mechanism is poorly understood [74]. Cardiac cushions in the AVC give rise to mitral (between the left ventricle and atrium) and tricuspid (between the right

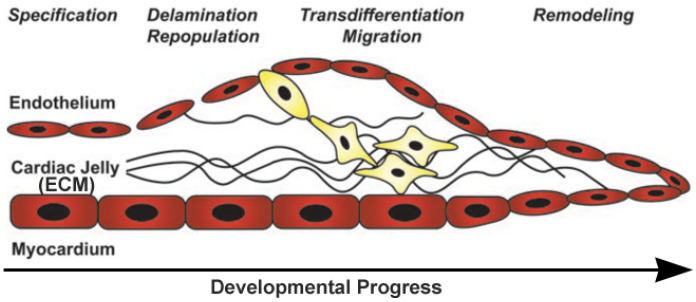

Figure 2. Overview of Cardiac Valve Development. A subset of endothelial cells at the future valve sites are specified to delaminate, differentiate, and migrate into the extracellular matrix (ECM) between myocardium and endocardium, also known as the cardiac jelly, through endothelial-to-mesenchymal transformation. Local swellings of cardiac jelly and mesenchymal cells are referred to as cardiac cushions. Later in valve development, cardiac cushions undergo a remodeling process to form thinly tapered cardiac valves. (Modified from [74]).

ventricle and atrium) valves, while the OFT cushions form aortic (between the left ventricle and aorta) and pulmonary (between the right ventricle and pulmonary artery) valves.

Information from *ex vivo* cushion explant studies have provided valuable insight into the EMT process during cardiac valvulogenesis, including the role of underlying myocardium in the valve forming regions and of soluble factors within the ECM [81, 82]. Also, knockout studies in mouse and large scale mutagenesis screens in zebrafish have complemented explant experiments. Multiple signaling molecules and other factors that are known to be involved in cardiac valve development can be integrated into several key pathways, and the hierarchy and interactions between them are actively being investigated.

Endocardial Cushion Formation

The first step of cardiac valve formation is to specify a subset of endocardial cells in the AVC and OFT regions for EMT. *Ex vivo* explant studies have shown that only 10-20% of

endocardial cells in the cushion-forming regions undergo EMT [74]. The exact mechanism initiating this event is not well understood, but the field property of the Notch pathway was proposed to be responsible [83]. Specified endocardial cells delaminate from the endothelial layer and migrate into the cardiac jelly to form the ECCs. This process is first induced by signaling molecules secreted from the underlying myocardium that inhibit expression of chamber-specific genes, but promote EMT of endocardial cells and synthesis of ECM components in the myocardium [65, 84, 85] (Fig.3). The subsequent EMT process requires signaling molecules from both the myocardium and endocardium [86] and disruption of any of these signaling pathways results in fatal cardiac valve abnormalities.

BMPs are members of the transforming growth factor (TGF) β superfamily and signal through Smad proteins. During cardiac valve development, BMPs function as the major myocardial-derived signals required for initiation of ECC formation and EMT. BMP2 and BMP4 are expressed in the myocardium of the AVC and OFT during valvulogenesis with BMP2 being expressed more strongly in the AVC and BMP4 in the OFT [84, 87, 88]. In the AVC myocardium, BMP2 promotes *Tbx2* expression that is necessary for suppression of chamber-specific gene expression and for increased ECM production [65, 89] (Fig.3). Cushion explant studies from chick and mouse showed that BMP2 can sufficiently increase *Tgfβ2* expression and initiate EMT in AVC endocardial cells [88, 90]. In mouse models, a single gene knockout of *Bmp6* or *Bmp7* does not produce any cardiac phenotype, but double mutants develop hypoplastic cardiac cushions [91]. Cardiac myocyte-specific deletion of *Alk3*, which encodes BMP receptor-Ia, also results in hypoplastic cardiac cushions [92]. However, a hypomorphic allele of BMP

receptor-II only affects the OFT valves, but not AVC valves [92], implying that differences exist between OFT and AVC valve formations even though both require BMP signaling.

TGFβs and BMPs are the most thoroughly studied signaling molecules during cardiac cushion formation. TGFβs signal through Smad2/3 while BMPs activate Smad1/5/8. TGFβ ligands and receptors are expressed in the AVC and OFT during ECC formation in mouse and chick [93], and TGFβ signaling activates *Snail/Slug* expression in endocardial cells [94]. They in turn negatively regulate expression of *VE-cadherin* and thereby decrease endocardial cell-cell adhesion, which allows endocardial cells to delaminate and migrate into the cardiac jelly [83, 94] (Fig.3).

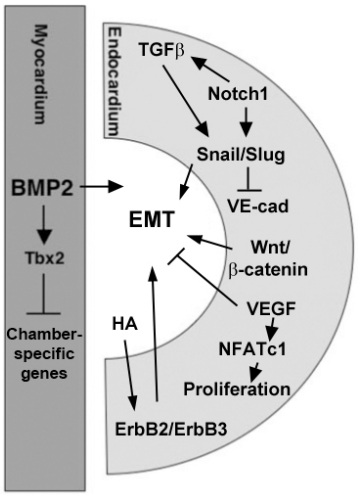

Figure 3. Signaling Events During Cardiac Cushion Formation. BMP2 increases ECM deposition and induces *Tbx2* expression, which inhibits chamber-specific gene expression. BMP2 and multiple endocardial-derived signals promote EMT. VEGF counteracts this process by maintaining endothelial characteristics of endocardial cells. VEGF also promotes endocardial cell proliferation through NFATc1. (Modified from [93]).

Wnt/β-catenin signaling also plays an important role during cardiac cushion formation. Endothelial-specific deletion of *β-catenin* in mice leads to cardiac cushion malformations due to defective EMT [95]. AVC cushion explants of these mutants fail to undergo EMT in response to TGFβ2. In zebrafish, mutants of Wnt signaling inhibitor *Adenomatous polyposis coli (APC)* develop excessive ECCs, while overexpression of APC or Dickkopf1, a secreted Wnt inhibitor, blocks cushion formation [96].

Another pathway implicated in endocardial EMT and cardiac cushion formation is Notch signaling. Knockout mice of *Notch1* or its associated transcription partner *RBP-Jκ (recombination signal-binding protein for immunoglobulin κJ region)* display hypoplastic cardiac cushions due to defective EMT [83]. These mice are initially able to form cushion swellings but they lack mesenchymal cells. Furthermore, injection of constitutively active Notch (NICD) in zebrafish embryos cause hypercellular cardiac cushion, while inhibition of Notch by DAPT, a γ-secretase inhibitor, prevent cushion formation [83]. Notch signaling was found to induce expression of *Snail* in endocardial cells of cushion-forming regions, thus facilitating the EMT process by reducing *VE-cadherin* expression in endocardial cells (Fig.3). Notch signaling was also shown to increase expression of *Tgfβ2* and multiple TGFβ receptors in the cardiac cushions, thus further promoting EMT. Mutations in Notch signaling components in humans are associated with abnormalities of semilunar (SL) valves (aortic and pulmonary valves), as exemplified in the cases of *Notch1* and *Jagged-1*, a Notch ligand and causative gene for Alagille syndrome [97, 98].

In addition to the signaling molecules mentioned above, ECM components and enzymes required for their synthesis are indispensible for cardiac cushion formation. The ECC is filled with glycosaminoglycans (GAGs) and proteoglycans that form a hydrated matrix for mechanical support and regulate ligand availability to growth factor receptors. For example, hyaluronic acid (HA), a GAG composed of alternating glucuronic acid and *N*-acetylglucosamine, interacts with numerous ECM proteins and regulates signaling events in the ECC [99]. Hyaluronan synthase 2 (Has2) is the major enzyme responsible for HA synthesis, and disruption of *Has2* in mice leads to complete loss of cardiac jelly

[100]. Endocardial cells of cushion-forming regions in these mice display a reduced capacity to undergo EMT *in vitro*, and this defect can be rescued by adding back HA or transfecting constitutively active Ras. Further study revealed that HA function is coupled to ErbB receptor signaling because addition of heregulin, a ligand for ErbB3, rescued defective EMT of *Has2*-null endocardial cells and restored phophorylation of ErbB2 and ErbB3 [101]. Moreover, *ErbB3* knockout mice die by E13.5 and exhibit hypoplastic cardiac cushions due to lack of proper EMT [102]. In zebrafish, the *jekyll* mutation disrupts *UDP-glucose dehydrogenase* gene that encodes an enzyme required for synthesis of glucuronic acid, a component of HA, and results in cardiac cushion defects [103, 104].

Maturation and Remodeling of Endocardial Cushions

After EMT, the ECC grows via cushion mesenchymal cell proliferation and continuous ECM production [80]. Proliferation of ECC mesenchymal cells after EMT is tightly regulated by multiple signals. BMP signaling is required not only for EMT but for growth of the ECC. *Bmp4* knockout mice exhibit hypocellular cardiac cushions that do not proceed to a remodeling stage [105, 106]. As mentioned above, double mutants for *Bmp6/Bmp7* and *Bmpr-II* mutants have hypoplastic OFT cushions while the AVC cushions are grossly normal [91, 107]. Conversely, mutation of the inhibitory Smad, *Smad6*, results in hyperplastic ECCs [108]. *In vitro* evidence indicates that BMP2 induces *Smad6* expression, thus providing a feedback loop to limit the amount of cells undergoing EMT and proliferation [109].

One of the key pathways that are important for regulating cushion mesenchymal cell proliferation during ECC maturation is the ErbB signaling pathway. Four Erb

proteins act as homo- or heterodimers and bind ligands including epidermal growth factor (EGF), heregulin/neuregulin family members, heparin-binding epidermal growth factor (HB-EGF), TGFα, amphiregulins, betacellulin, and epiregulin [110]. Different combinations of ErbB receptors bind ligands with different affinities and function at different stages of cardiac valve morphogenesis. Mice that are homozygous for an *Egfr* hypomorphic allele display hyperplastic OFT cushions due to over-abundant mesenchymal cells, without affecting the AVC cushions [111]. This phenotype is enhanced by heterozygosity for *Ptpn11*, a gene encoding the tyrosine phosphatase Shp2, which is a positive downstream regulator of EGFR. Gain-of-function mutations of *Ptpn11* are also associated with more than 50% of Noonan syndrome patients who often have pulmonic stenosis [75]. Endothelial-specific expression of activating Shp2 in mice results in increased extracellular signal-activated kinase (ERK) 1/2 activation and increased proliferation of ECC mesenchymal cells [112].

Knockout mice of ErbB ligands corroborated the requirement of ErbB signaling during ECC remodeling. In the developing mouse, HB-EGF, a ligand for ErbB1/EGFR and ErbB4, is strongly expressed in the endocardium overlying the cushion-forming regions, and *Hb-egf* knockout mice develop enlarged cardiac valves and die right after birth [113]. Consistent with this result, deficiency of TACE/ADAM17, an enzyme converting inactive pro-HB-EGF to active HB-EGF, produces identical cardiac phenotype with *Hb-egf* mutation in mice [113]. In these mice, endocardial EMT initiates normally but mesenchymal proliferation proceeds unchecked.

A number of studies implicated the role of vascular endothelial growth factor (VEGF) during valvulogenesis. VEGF is a pleiotropic factor that regulates endothelial

cell proliferation, survival, and chemotaxis [114]. It is expressed throughout endocardial cells at E9.0 but its expression becomes restricted to endocardial cells in the valve-forming regions at the beginning of ECC formation [115, 116]. Experiments from chick, mouse, and zebrafish demonstrated that VEGF signaling promotes endocardial cell proliferation in the cushion-forming regions to provide an enough pool of endocardial cells for cushion formation [115-117]. It also inhibits endocardial cell EMT by promoting endocardial cells to maintain endothelial cell characteristics (Fig.3). Therefore, the VEGF expression level must be tightly regulated during cardiac valvulogenesis because both over- and underexpression of *Vegf* block ECC formation.

During cardiac cushion formation, *Nuclear factor of activated T cells cytoplasmic 1 (NFATc1)* is expressed in endocardial cells in the AVC and OFT, but its expression disappears in cells that have undergone EMT [118, 119]. *Nfatc1* knockout mice fail to develop the ECC and die by E13.5. Further experiments showed that VEGF promotes endocardial cell proliferation through activation of *Nfatc*1, and this effect is specific to cardiac cushion endothelial cells [120] (Fig.3). *Nfatc1* expression is maintained in valve endothelial cells even after birth, suggesting its role in adult valve homeostasis [120].

Chemokine Receptor CXCR7

CXCR7 (formerly known as RDC1) is a recently deorphanized seven transmembrane G protein-coupled receptor (GPCR). *Rdc1* was first cloned from a dog cDNA library as a putative GPCR for the vasoactive intestinal peptide (VIP) hormone [121, 122]. However, the binding of VIP to RDC1 was revoked soon after discovery [123, 124]. RDC1 was

then proposed as a chemokine receptor based on its amino acid sequence similarity and identity to CXCR2, and its chromosomal location [125]. *Rdc1* is positioned in the vicinity of *Cxcr4*, *Cxcr2*, and *Cxcr1* on mouse chromosome 1 and human chromosome 2. The proposal that RDC1 might be a chemokine receptor was further supported by phylogenetic studies and its ability to act as a co-receptor for human immunodeficiency viruses (HIVs), which is a feature of many chemokine receptors [126-128]. Also, it is evolutionarily highly conserved between species, suggesting an important physiological role of this receptor [129].

Designation of RDC1 as CXC chemokine receptor 7 (CXCR7) was made on the basis of its high affinity to chemokines CXCL12/SDF1 (stromal cell-derived factor 1) and CXCL11/I-TAC [130, 131]. This discovery challenges the notion that CXCL12 has a monogamous relationship with CXCR4, as suggested by the nearly identical phenotypes of CXCL12 and CXCR4 knockout mice [132-135]. However, the significance of ligand binding to CXCR7 has been elusive since CXCR7 does not appear to trigger typical chemokine responses like chemotaxis and Ca^{2+} mobilization, or activate intracellular signaling, such as mitogen-activated protein kinase (MAPK) or phosphoinositide 3 kinase (PI3K)/protein kinase B (PKB) pathways [130, 131, 136-141]. Most chemokine receptors have a DRYLAIV motif at the N-terminus of the second intracellular loop, which is necessary but not sufficient for coupling to Gi proteins [129]. CXCR7 has two amino acid changes in this motif (A to S and V to T), but these changes can be seen in other chemokine receptors, too. Even though internalization of CXCR7 was observed upon CXCL12 binding, this process is known to be G protein independent [131, 137, 142].

The first clue about CXCR7 function came from the study of leukocytes. Survival and efficient differentiation of B cells into plasma cells are correlated with CXCR7 levels on the cell surface [140]. Interestingly, the expression of *Cxcr7* is inversely proportional to CXCR4 activity on B cells. More evidence of its function in cell survival and proliferation has followed. For example, fibroblast cells overexpressing *Cxcr7* form tumor in nude mice [143]. In addition, elevated *Cxcr7* expression has been reported in numerous tumor cell lines, primary human tumors, and tumor vascular endothelial cells, and *Cxcr7* expression is often correlated with tumor growth or aggressiveness [131, 144-148]. CXCR7 is also important in CXCR4-mediated transendothelial migration of tumor cells but not in intra-tissue chemotaxis [149].

Recently, CXCR7 has been implicated in development of zebrafish. During CXCR4-mediated migration of primordial germ cells and lateral line primordium, CXCR7 creates an essential CXCL12 gradient by sequestering and internalizing CXCL12 [137, 139, 150].

In summary, CXCR7 is an atypical chemokine receptor that may play a role in either cell migration or cell survival and proliferation. Although the downstream pathway of CXCR7, if any, has not been identified, its function seems to be associated with CXCR4 directly or indirectly. In some settings, CXCR7 may form a heterodimer with CXCR4 and modulate certain aspects of CXCR4 functions [136, 151-153]. In other settings, CXCR7 may act as a decoy or scavenger receptor to regulate the extracellular CXCL12 level available to CXCR4 as stated above [154]. However, CXCR7 may have CXCR4-independent functions as it is able to promote cell survival and adhesion in the absence of CXCL12 [131, 143, 147]. Existence of CXCR7 ligand(s) distinct from

CXCL12 and CXCL11 was reported, albeit unknown, which might explain the CXCR4-independent functions [140].

Hypothesis and Specific Aims

Cxcr7 knockout mice die perinatally possibly due to cardiac defects. Newborn pups are cyanotic indicating insufficient blood supply to peripheral tissues, and their hearts are enlarged at birth implying pressure overload. The unexpected cardiac phenotypes of *Cxcr7* mutants led to the hypothesis that CXCR7 might have an important function during heart development. To test this hypothesis, I tested *Cxcr7* expression pattern in the heart and histologically analyzed mutant hearts, which revealed thickening of semilunar valves at the valve remodeling stage. To determine the etiology of semilunar valve thickening, I tested proliferation and apoptosis rates of cushion mesenchymal cells, which showed increased proliferation of mesenchymal cells. To identify the mechanism of increased proliferation, I checked the level of several signaling pathways controlling valve mesenchymal cell proliferation during valve remodeling. To find out the cell type in which CXCR7 function is important, endothelial cell-specific *Cxcr7* knockout mice were generated and analyzed, histologically and functionally.

CHAPTER TWO

LOSS OF CXCR7 RESULTS IN PERINATAL LETHALITY DUE TO THICKENING OF CARDIAC SEMILUNAR VALVES

Introduction

VSD is one of the most common CHDs and can be derived from two different origins, muscular and membranous. The muscular VSD can be present in any muscular part of the ventricular septum and the causative genes are mostly involved in myocardial morphogenesis, such as *Nkx2-5*, *Tbx5*, and *Gata4*. On the other hand, the membranous VSD has an endocardial or neural crest origin and accounts for about 80% of all VSDs. The membranous part of the ventricular septum develops from the atrioventricular ECCs [155], and mutations of genes involved in ECC morphogenesis often affect this part of the septum.

As explained previously, cardiac NCCs originate from the otocyte and somite 3, and are essential during the aorticopulmonary septum and OFT lengthening by the SHF [156]. Cardiac defects resulted from cardiac NCC abnormalities include OFT septal defect and overriding aorta, among others [157]. Overriding aorta is an alignment defect that is associated with abnormal looping during early heart development, and is always accompanied by a VSD [158]. A variety of environmental signals are required for NCC specification, migration, proliferation, differentiation, and survival (reviewed in [159]).

A broad microarray screen to examine the gene expression profile of marginal zone B cells showed that *Cxcr7* is highly expressed in marginal zone B cells but not in mature or immature B cell populations (Crawford, D. and Behrens, T.W., unpublished

data). To test whether *Cxcr7* is required for the migration of marginal zone B cells, the *Cxcr7* conditional allele was generated in mice in which the entire coding region of *Cxc7* is flanked by *loxP* sites ($Cxcr7^{flox}$, Appendix A). Subsequent recombination by the *Cre* transgene deletes *Cxcr7* either ubiquitously or tissue specifically depending on the kind of *Cre* used.

Results

Perinatal Lethality of Cxcr7 Knockout Mice

$Cxcr7^{flox}$ mice were crossed with *deleter Cre* mice [160] to allow ubiquitous *Cxcr7* deletion, and F1 mice were out-crossed with C57BL/6 mice to establish a stably transmitting mouse line with deletion of *Cxcr7*, $Cxcr7^{+/-}$. When $Cxcr7^{+/-}$ mice were inter-crossed, no $Cxcr7^{-/-}$ mice were found at weaning (Fig. 1A). A normal Mendelian ratio was observed at E16.5 (Fig. 1A) without abnormalities in size, color, or gross anatomy. About a third of E18.5 $Cxcr7^{-/-}$ mice delivered by cesarean birth were dead. The remaining mice died shortly after birth; most were cyanotic and gasped for breath, but the phenotype was variable. For example, in a litter of eight mice, one of three $Cxcr7^{-/-}$ mice died at or just before birth and appeared to have a catastrophic circulatory failure in late development, as it was completely white within a blood-filled embryonic sac (mouse 18-12, Fig. 1B). The second appeared anatomically normal but never breathed (mouse 18-10, Fig. 1B), and the third gasped and remained cyanotic before dying within 1 hr after birth (mouse 18-6, Fig. 1B). Some $Cxcr7^{-/-}$ mice appeared normal and robust at birth but then showed signs of stress, such as gasping for breath, and died suddenly.

To identify the cause of death of the *Cxcr7*$^{-/-}$ mice, I harvested E18.5 embryos from intercrosses of *Cxcr7*$^{+/-}$ mice, and examined the internal organs. In *Cxcr7*$^{-/-}$ embryos, the lungs appeared normal and were able to inflate. All other internal organs looked grossly normal except the hearts, which were slightly larger than the hearts of wild-type littermates and often had dysmorphic shapes rather than a normal cone shape (Fig 1C, the third panel). Occasionally, the mutants had aortas sprouting from the right side of the heart instead of the left side (Fig. 1C, the second panel), or had dilated atria (Fig. 1C, the third panel).

Expression Pattern of Cxcr7 in Mice

The cyanotic pups, enlarged hearts, OFT patterning defect, and dilated atria all indicate possible cardiac defects in *Cxcr7*$^{-/-}$ mice. Before analyzing more detailed cardiac phenotypes, I examined the expression pattern of *Cxcr7* in mouse. I performed whole-mount *in situ* hybridization with E10.5 mouse embryos, and *Cxcr7* was expressed at high levels in the prosencephalon, especially in the nasal process, and a part of the rhomboencephalon, and expressed at lower levels in the neural tube, somites, and heart (Fig. 2A). The result from a postnatal (P) day 1 mouse shows that *Cxcr7* is more broadly expressed in various tissues, including the heart (Fig. 2B). To analyze the regional expression pattern of *Cxcr7* in the heart, I made transverse sections of E10.5 mouse embryos after the whole-mount *in situ* staining. *Cxcr7* was mainly expressed in endocardial cells and their ECC mesenchymal cell derivatives in both the OFT and AVC (Fig. 2C–F), and expressed to a lesser degree in myocardial cells (Fig. 2C, E).

Thickening of Semilunar Valves and Ventricular Septal Defect in Cxcr7 Knockout Mice

In addition to abnormal heart morphologies of the E18.5 *Cxcr7*$^{-/-}$ embryos, the expression of *Cxcr7* in the heart corroborated the hypothesis that *Cxcr7* might have an important function during heart development. To examine the cardiac phenotype of the *Cxcr7*$^{-/-}$ mouse embryos more closely, transverse and coronal sections of the E18.5 *Cxcr7*$^{-/-}$ hearts were made. Comparison of the cardiac sections between wild-type and mutant embryos revealed thickened SL valves in all *Cxcr7*$^{-/-}$ embryos (Fig. 3A-H). However, the tricuspid and mitral valves were normal (Fig. 3I, J). One third of the embryos (n=9) had VSDs in a membranous portion of the septum, and 22% had overriding aorta, in which the aorta is positioned on top of the ventricular septum (Fig. 3H).

To determine when the OFT endocardial cushion/SL valve thickening occurs during development, heart sections were made at progressive mouse embryonic stages. Until around E14.0, there was no apparent difference in the size of the OFT endocardial cushions (Fig. 4A-C and 4E-G). However, at E15.5, when wild-type valve thinning into leaflets had already begun, *Cxcr7*$^{-/-}$ valves were still thick, indicating defects in SL valve remodeling (Fig. 4D, H).

Migration of Cardiac Neural Crest cells in Cxcr7 Knockout Mice

Although *Cxcr7* is not expressed in NCCs (Fig. 2A), and the structure of pharyngeal arch arteries was normal in *Cxcr7*$^{-/-}$ embryos (data not shown), the valve thickening was observed only in the OFT valves, and VSD and overriding aorta were present in some

cases. Therefore, I speculated that CXCR7 might be involved in the migration of cardiac NCCs as *Cxcr7* is expressed in the neural tube (Fig. 2A). To test this possibility, *Cxcr7*$^{-/-}$ embryos were stained for *cellular retinoic acid binding protein 1* (*Crabp1*), a neural crest marker, at around E10.5. The amounts of cardiac NCCs migrating through pharyngeal arches 3, 4, and 6 were similar between the wild-type and *Cxcr7*$^{-/-}$ embryos (Fig. 5A, B).

Discussion

Deletion of *Cxcr7* in mice resulted in perinatal lethality with cardiac defects. The death most likely resulted from insufficient blood flow to the body caused by SL valve stenosis, a condition that can cause severe cardiac dysfunction in human newborns as well. Enlarged hearts and dilated atria are likely to be the secondary effects of pressure overload in the ventricles caused by SL valve stenosis.

Thickening of ECC/valve primordia can originate from either myocardial or endocardial defects. Expression of *Cxcr7* in endocardial and ECC mesenchymal cells but little or no expression in myocardial cells implies its function in the ECC. Normal development of atrioventricular valves indicates that *Cxcr7* might not be required for development of tricuspid and mitral valves, or its loss might be compensated by other proteins in the AVC. The membranous ventricular septum is derived from the AVC cushions, and the membranous VSD in the *Cxcr7*$^{-/-}$ mice suggests that *Cxcr7* may still have a role in the AVC cushion.

Valve thickening can result from problems in various steps of valve development, such as specification, EMT, growth, or remodeling. The OFT sections of *Cxcr7*$^{-/-}$ embryos at various developmental stages revealed that the *Cxcr7*$^{-/-}$ hearts have defects

during the SL valve remodeling process, as the sizes of the OFT ECCs in the *Cxcr7*$^{-/-}$ hearts are comparable to those of the wild-type hearts until E14.0.

Overriding aorta and membranous VSD in the *Cxcr7*$^{-/-}$ mice suggests that *Cxcr7* deficiency might affect cardiac NCCs [156]. However, *Cxcr7* is not expressed in NCCs and defects in OFT septation or patterning of pharyngeal arch arteries were not observed. Even though the link between CXCR7 and cardiac NCCs cannot be ruled out, at least the migration of cardiac NCCs is not affected by *Cxcr7* deficiency.

Materials and Method

Mating of Mice and Genotyping

Cxcr7$^{+/-}$ mice were kindly provided by Dr. Behrens, T.W. (University of Minnesota, Minneapolis, MN). *Cxcr7*$^{+/-}$ mice were intercrossed to produce *Cxcr7*$^{-/-}$ embryos. E18.5 embryos were obtained from cesarean sections of pregnant females. Earlier stage embryos were dissected under the microscope using forceps after uteri were obtained from the pregnant females at desired developmental stages. Noon of the day when a virginal plug was observed was set to E0.5. DNA was extracted from the yolk sac and polymerase chain reaction (PCR) was performed for genotyping. Primers for genotyping are: wild-type forward –CCG CTA TCT CTC CAT CACC; wild-type reverse – GAT CTT CCG GCT ACT GTGC; knockout forward – CTG CCT CTC TTG GGA ATGT; knockout reverse – CTC TCT GGC CGT TCT CTC.

Whole-mount and Section in Situ Hybridization

Section *in situ* hybridization for P1 mouse was performed by Phylogeny (Columbus, OH). Mouse tissue was frozen, cut into 6–12-µm sections, mounted on gelatin-coated slides, and fixed in 4% formaldehyde. The cRNA probe for *Cxcr7* was synthesized *in vitro* according to manufacturer's conditions (Ambion) and labeled with ^{35}S-UTP (Amersham). Sections were hybridized overnight at 55^{o}C with ^{35}S-labeled cRNA probe (50–80,000 cpm/µl).

Whole-mount *in situ* hybridization for *Cxcr7* and *Crabp* mRNA was performed with E10.5–E11.0 embryos. Embryos were fixed in 4% formaldehyde overnight and kept in 100% methanol at –20^{o}C until use. Embryos were treated by proteinase K (Roche) for 15-20 min and re-fixed with 4% formaldehyde/0.2% glutaraldehyde for 20min. Embryos were then pre-hybridized at 65^{o}C for 1-2 hrs without riboprobe before hybridization was performed at 65^{o}C overnight. Hybridization buffer consists of 50% formamide, 5x SSC, 0.5 mg/ml salmon sperm DNA (Invitrogen), 0.1% Tween-20 (Sigma), 50µg/ml heparin (Sigma), 200µg/ml yeast tRNA (Ambion), citric acid to pH6.0. After the hybridization, embryos were washed extensively with post-hybridization buffer (hybridization buffer without salmon sperm DNA, heparin, and yeast tRNA) and then with PBT.3 (PBS/0.3% triton X-100). Embryos were blocked by Genius blocking reagent (Roche), and then incubated with anti-DIG-AP antibody (Roche) at 1:2000 dilution for 2hrs at room temperature (RT). Embryos were washed with PBT.3, then PBT.5, and finally AP buffer (100mM Tris-HCl pH9.5, 100mM NaCl, 50mM $MgCl_2$, 0.1% Tween-20, 1mM levamisole (Sigma)). Embryos were stained with BM purple substrate (Roche) at RT, overnight, wrapped in aluminum foil to block light. Riboprobes were labeled with DIG.

Histology

Embryonic hearts at various stages were embedded in paraffin, cut into 8–10μm sections, deparaffinized, and stained with hematoxylin and eosin for histological analysis. E18.5 hearts were sectioned transversely to have a top view and coronally to have a frontal view. Earlier stage sections were made coronally to observe the OFT better.

Figures

Figure 1

A

3 wks	+/+	+/-	-/-
number	25	44	0
%	36%	64%	0%

e16.5	+/+	+/-	-/-
number	12	21	10
%	28%	49%	23%

B

C

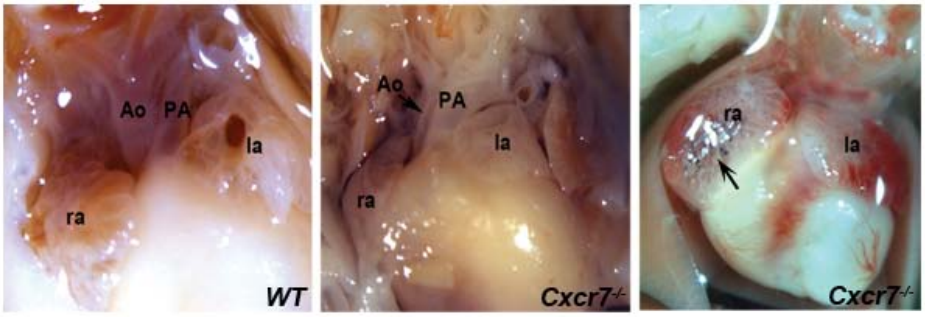

Figure 1. Perinatal lethality of *Cxcr7* knockout mice. (A) Genotypes of offspring from *Cxcr7*$^{+/-}$ x *Cxcr7*$^{+/-}$ crosses at weaning and at E16.5. **(B)** Six of eight E18.5 mice from a single (*Cxcr7*$^{+/-}$ x *Cxcr7*$^{+/-}$) litter, photographed less than 1 hr after cesarean birth. Identifier and genotypes are shown for each mouse. **(C)** Frontal views of E18.5 wild-type and *Cxcr7*$^{-/-}$ hearts. In 22% of the *Cxcr7*$^{-/-}$ hearts, the aorta was misaligned and coming out of the right side (arrow in the second panel). About in 30% of the *Cxcr7*$^{-/-}$ hearts, either the left or right atrium is enlarged (arrow in the third panel). Ao, aorta; PA, pulmonary artery; ra, right atrium; la, left atrium. (A) and (B) were produced by Crawford, D., University of Minnesota, MN.

Figure 2

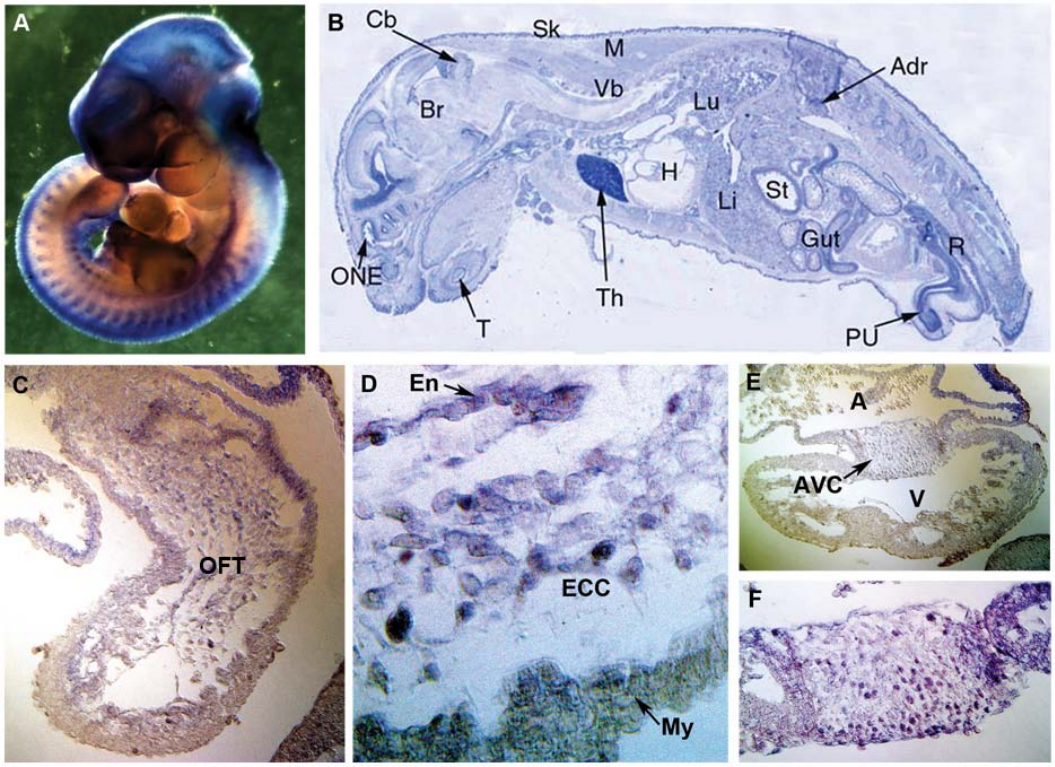

Figure 2. Expression pattern of *Cxcr7* mRNA in developing mouse heart. (A) Whole-mount *in situ* hybridization was carried out with digoxigenin (DIG)-labeled *Cxcr7* riboprobe at E10.5. *Cxcr7* mRNA is expressed in the prosencephalon, rhombencephalon, somites, neural tube, and heart at this stage. **(B)** Section *in situ* hybridization image of sagittally sectioned P1 mouse. *Cxcr7* is expressed in various tissues, including the brain, thymus, heart, stomach, and liver. Adr, adrenal gland; Br, brain; Cb, cerebellum; H, heart; Li, liver; Lu, lung; M, muscle; ONE, optic nerve ending; PU, penile urethra; R, rectum; Sk, skin; St, stomach; T, tooth; Th, thymus; Vb, vertebrae (Phylogeny, Columbus, OH). (**C–F)** Transverse sections were made after whole-mount *in situ* hybridization at E10.5. *Cxcr7* is expressed in endocardial and ECC mesenchymal cells in both the OFT (C-D) and AVC (E-F). *Cxcr7* expression in myocardial cells is much weaker than that of endocardial cells. (D) and (F) are high-magnification images of (C) and (E), respectively. OFT, outflow tract; En, endocardium; ECC, endocardial cushion; My, myocardium; A, atrium; V, ventricle; AVC, atrioventricular canal.

Figure 3

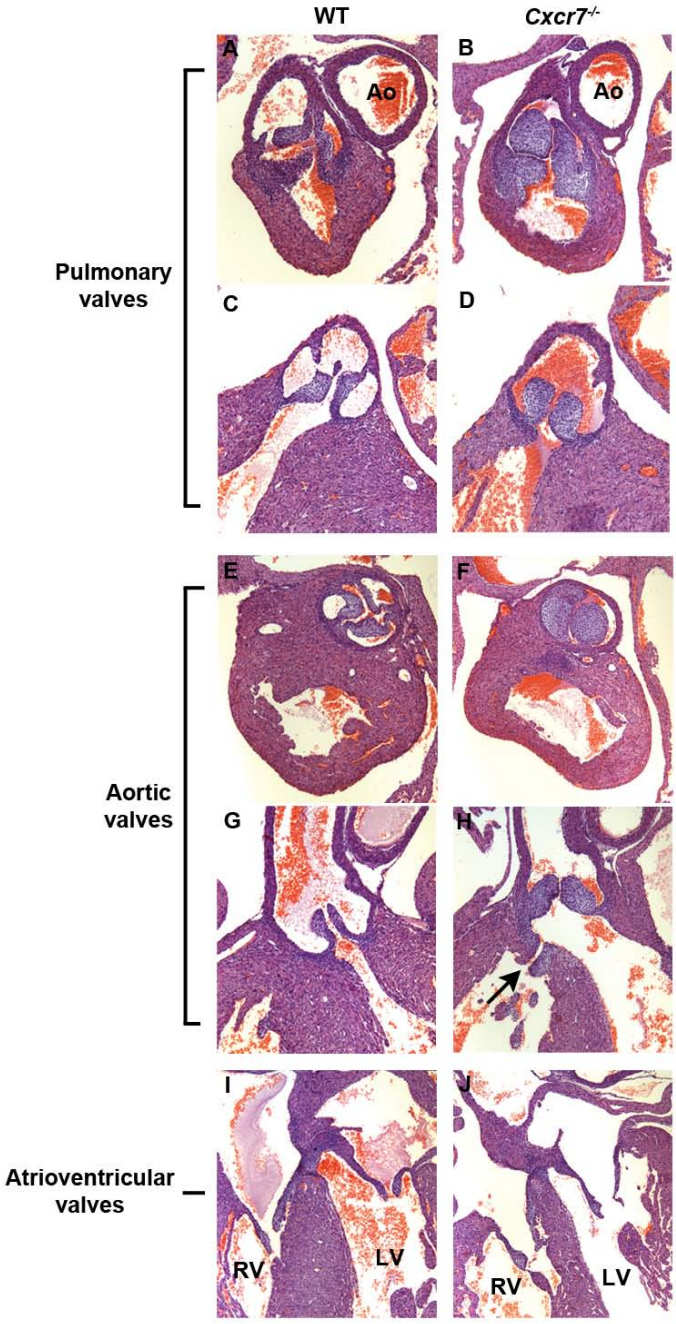
WT
Cxcr7-/-
A
B
Ao
Ao
Pulmonary valves
C
D
E
F
Aortic valves
G
H
I
J
Atrioventricular valves
RV
LV
RV
LV

Figure 3. *Cxcr7*$^{-/-}$ embryos have enlarged SL valves and occasional VSD or overriding aorta. (**A–J)** Sections of E18.5 mouse embryonic hearts were stained by hematoxylin-eosin. *Cxcr7*$^{-/-}$ embryos have thick pulmonary and aortic valves but normal tricuspid and mitral valves. VSD was observed in 33.3% (n=9) of cases (arrow in H). Transverse sections are shown in A, B, E, and F. Coronal sections are shown in C, D, G, H, I, and J. Ao, aorta; RV, right ventricle; LV, left ventricle.

Figure 4

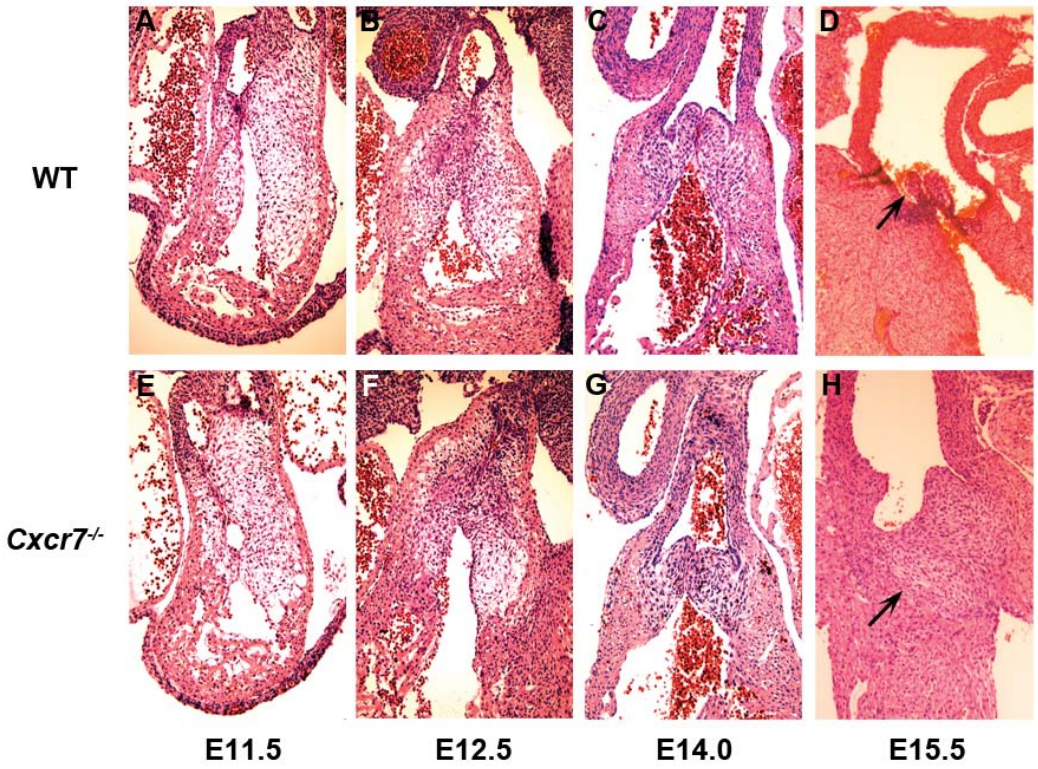

Figure 4. The OFT endocardial cushions in *Cxcr7*$^{-/-}$ embryos fail to undergo valve remodeling in mice. (**A-H)** Coronal sections were made from the hearts of wild-type and *Cxcr7*$^{-/-}$ embryos at various developmental stages. The size and cell number of the OFT endocardial cushions or SL valve primordia were not significantly different between the wild-type and *Cxcr7*$^{-/-}$ embryos until E14. Difference in the size of the SL valves became apparent at around E15.5, when the valves were undergoing a remodeling process and formed thin leaflets in wild-type hearts, but remained enlarged in *Cxcr7*$^{-/-}$ hearts (arrows in D and H).

Figure 5

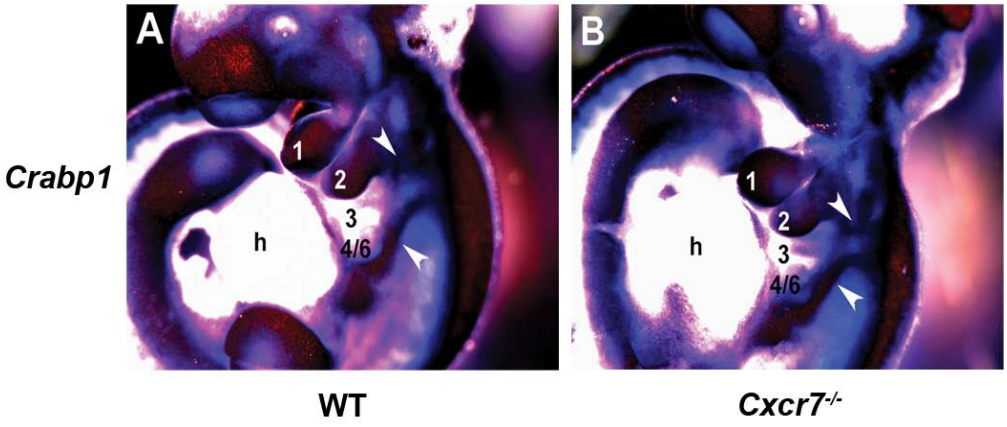

Figure 5. Deletion of *Cxcr7* does not affect migration of cardiac neural crest cells. **(A-B)** Whole-mount *in situ* hybridization was performed with wild-type and *Cxcr7*$^{-/-}$ embryos at E10.5 by a DIG-labeled *Crabp1* riboprobe. Cardiac neural crest cell migration is not affected in the *Cxcr7*$^{-/-}$ embryos. Arrowheads indicate migrating neural crest cells through pharyngeal arches 3, 4, and 6. h, heart.

CHAPTER THREE

CXCR7 IS REQUIRED IN ENDOCARDIAL-DERIVED CELLS TO REGULATE CARDIAC VALVE REMODELING

Introduction

Soon after birth, cardiomyocytes withdraw from the cell cycle and subsequent growth of the heart occurs through hypertrophy, rather than hyperplasia [16]. Cardiac hypertrophy is an adaptive response to stress that includes hypertension, pressure overload, endocrine disorder, myocardial infarction, and contractile dysfunction caused by defects of structural proteins. There are two types of hypertrophic phenotypes: (1) concentric hypertrophy due to pressure overload, which is characterized by the addition of sarcomeres in parallel to make the ventricular wall thicker without affecting the lumen size, and (2) eccentric hypertrophy due to volume overload, during which sarcomeres are added in series to make the ventricular lumen bigger [161]. The heart with concentric hypertrophy maintains normal systolic functions such as an ejection fraction, but has defective diastolic functions. Meanwhile, the heart with eccentric hypertrophy has defective systolic functions. Both types of hypertrophy can later progress to dilated cardiomyopathy through a mechanism that may involve apoptosis, necrosis, or fibrosis, and can lead to heart failure, cardiac arrhythmia, and sudden death [162].

Results

Endocardial-Specific Deletion of Cxcr7 in Mice Results in SL Valve Stenosis

The expression pattern of *Cxcr7* in developing mouse embryos suggests its function in endocardial cells. To confirm this hypothesis and to examine the role of *Cxcr7* in the adult heart, I deleted *Cxcr7* specifically in all endothelial cells using the *Tie2-Cre* transgene. *Tie2-Cre;Cxcr7*$^{flox/-}$ mice survived normally after birth and were fertile. However, when examined at 6 months of age, they had massive cardiac hypertrophy (Fig. 1A).

To determine whether *Tie2-Cre;Cxcr7*$^{flox/-}$ mice have similar SL valve stenosis to *Cxcr7*$^{-/-}$ mice, I examined histological sections at the level of SL valves. Indeed, the SL valves of *Tie2-Cre;Cxcr7*$^{flox/-}$ mice were thicker than those of wild-type mice, and the difference was more dramatic in the aortic valves (Fig. 1B-E). As in the *Cxcr7*$^{-/-}$ hearts, the tricuspid and mitral valves were normal in *Tie2-Cre;Cxcr7*$^{flox/-}$ mice (data not shown). The SL valves in mutants were often fused at their bases, which prevents dynamic opening and closing of the valves (Fig. 1E). These results suggest that the *Cxcr7* expression in endocardial cells and their valve mesenchymal derivatives is necessary to prevent thickening of the SL valves.

Tie2-Cre;Cxcr7$^{flox/-}$ *Mice Develop Cardiac Hypertrophy*

Cross sections of age-matched wild-type and *Tie2-Cre;Cxcr7*$^{flox/-}$ hearts revealed much thicker ventricular walls in mutant hearts, but similar sizes of ventricular cavities (Fig. 2A). Examination of myocardial structures of the *Tie2-Cre;Cxcr7*$^{flox/-}$ hearts at high magnification revealed greatly enlarged cardiomyocytes, cellular disarray, and increased

intercellular space (Fig. 2B, C). At 6 months of age, the mutant mice had substantial fibrosis, marked by Masson's trichrome staining, in the myocardium and around microvessels in the heart; little fibrosis was detected in the wild-type mice (Fig. 2D, E). On the other hand, calcium deposition was not observed in the mutant SL valves when tested by Von Kossa staining (Appendix B).

Echocardiographic analysis of cardiac function at 6 months of age showed no difference in fractional shortening or ejection fraction between the *Tie2-Cre;Cxcr7*$^{flox/-}$ and wild-type mice (Fig. 3A), but the left ventricular posterior wall was about 1.4-fold thicker in the *Tie2-Cre;Cxcr7*$^{flox/-}$ mice (Fig. 3B). These features are consistent with concentric hypertrophy caused by pressure overload [163]. Results of other echocardiographic measurements can be found in Appendix C.

Discussion

Endothelial cell-specific deletion of *Cxcr7* bypassed the perinatal lethality but caused the similar cardiac defects, SL valve stenosis, to ubiquitous deletion of *Cxcr7* in mice. This indicates there might be other attributes that caused death of *Cxcr7*$^{-/-}$ mice. Given the broad expression pattern of *Cxcr7*, it may have important functions during development in other organs even though other organs looked grossly normal in the *Cxcr7*$^{-/-}$ mice at E18.5.

The valve thickening phenotype of *Tie2-Cre;Cxcr7*$^{flox/-}$ mice was more severe in the aortic valves, and the leaflets were often fused at their bases. The reason for difference between the aortic and pulmonary valves is not clear, but the phenotype may suggest that aortic valve development is more sensitive to the loss of *Cxcr7*. Alternatively,

the pulmonary valve defects might be normalized in adults through an unknown mechanism, as the size was not different between the aortic and pulmonary valves at E18.5 in *Cxcr7*$^{-/-}$ embryos.

It is interesting that I did not observe VSD or overriding aorta in the *Tie2-Cre;Cxcr7*$^{flox/-}$ mice. It might be simply because I examined fewer *Tie2-Cre;Cxcr7*$^{flox/-}$ mice than *Cxcr7*$^{-/-}$ mice, and low penetrance of these phenotypes (33% for VSD and 22% for overriding aorta) prevented me from encountering them in the *Tie2-Cre;Cxcr7*$^{flox/-}$ mice. Another possibility is that imperfect efficiency of the *Tie2-Cre* and consequently incomplete recombination of *loxP* sites in endothelial lineages prevented these phenotypes to show up. Otherwise, expression of *Cxcr7* in non-endothelial derivatives might be important for the formation of the membranous ventricular septum and OFT patterning.

SL valve stenosis imposes pressure overload on the heart and can lead to cardiac hypertrophy. Consistent with this, 6-month-old *Tie2-Cre;Cxcr7*$^{flox/-}$ mice had massive cardiac hypertrophy characteristic of concentric hypertrophy, even though diastolic dysfunction was not observed when the ventricular lumen size was measured during diastole and systole by echocardiography (Appendix C).

Prolonged cardiac hypertrophy can lead to fibrosis of the ventricles and I found that the *Tie2-Cre;Cxcr7*$^{flox/-}$ mice had substantial fibrosis in the heart. Patients with bicuspid aortic valves often have calcified valves due to the activation of bone development program [164]. Even though I did not observe the bicuspid aortic valves in the *Tie2-Cre;Cxcr7*$^{flox/-}$ mice, because of the massively enlarged aortic valves with occasional leaflet fusions at the bases, I speculated that these mice might have calcific

aortic valves. However, measurement of calcium deposition in the *Tie2-Cre;Cxcr7*$^{flox/-}$ aortic valves showed very little calcium accumulation in the aortic valves (Appendix B). Combined with lack of diastolic dysfunction, this result might indicate that 6 months was too early to detect more advanced phenotypes of hypertrophy and aortic valve defects.

Materials and Methods

Generation of Tie2-Cre;Cxcr7$^{flox/-}$ *Mice and Genotyping*

Tie2-Cre mice were purchased from the Jackson laboratory. Either (*Tie2-Cre;Cxcr7*$^{+/-}$ x *Cxcr7*$^{flox/flox}$) or (*Tie2-Cre;Cxcr7*$^{flox/+}$ x *Cxcr7*$^{+/-}$) crosses were set up to obtain *Tie2-Cre;Cxcr7*$^{flox/-}$ mice. PCR primers used to distinguish wild-type and floxed alleles are: forward, 5' – CAAACCCGTGAACAAGG; reverse: 5' – CTCTCTGGCCGTTCTCTC. Primers for *Tie2-Cre* are: forward, 5' – CGATGCAACGAGTGATGAGG; reverse, 5' – CGCATAACCAGTGAAACAGC.

Histological Analysis

Whole hearts were taken from 6-month-old wild-type and *Tie2-Cre;Cxcr7*$^{flox/-}$ mice and were embedded in paraffin, cut into 8–10μm sections, deparaffinized, and stained with hematoxylin and eosin for histological analysis.

Masson's Trichrome Staining

For Masson's trichrome staining, 6-month-old hearts from wild-type and *Tie2-Cre;Cxcr7*$^{flox/-}$ mice were embedded in paraffin and transversely sectioned. Deparaffinized sections were dipped sequentially into Weigert's iron hematoxylin

working solution for 10 min, Biebrich scarlet-acid fuchsin solution for 15 min, phosphomolybdic-phosphotungstic acid solution for 15 min, aniline blue solution 5–10 min, and 1% acetic acid solution for 2–5 min.

Echocardiography

Various cardiac parameters were assessed by M-mode and power Doppler mode in 6-month-old wild-type and *Tie2-Cre;Cxcr7*$^{flox/-}$ mice anesthetized with 1.75% isoflurane. Core temperature was maintained at 37–38°C, and scans were performed in a random-blind fashion. Each mouse underwent three separate scans on three different days. Values were averaged from three scans for each mouse. Fractional shortening and ejection fraction were calculated from left ventricular end systolic dimension (LVESD) and left ventricular end diastolic dimension (LVEDD). Fractional shortening (%) = LVEDD – LVESD/LVEDD x 100. Ejection fraction (%) = $LVEDD^2 – LVESD^2/LVEDD^2$ x 100.

Figures

Figure 1

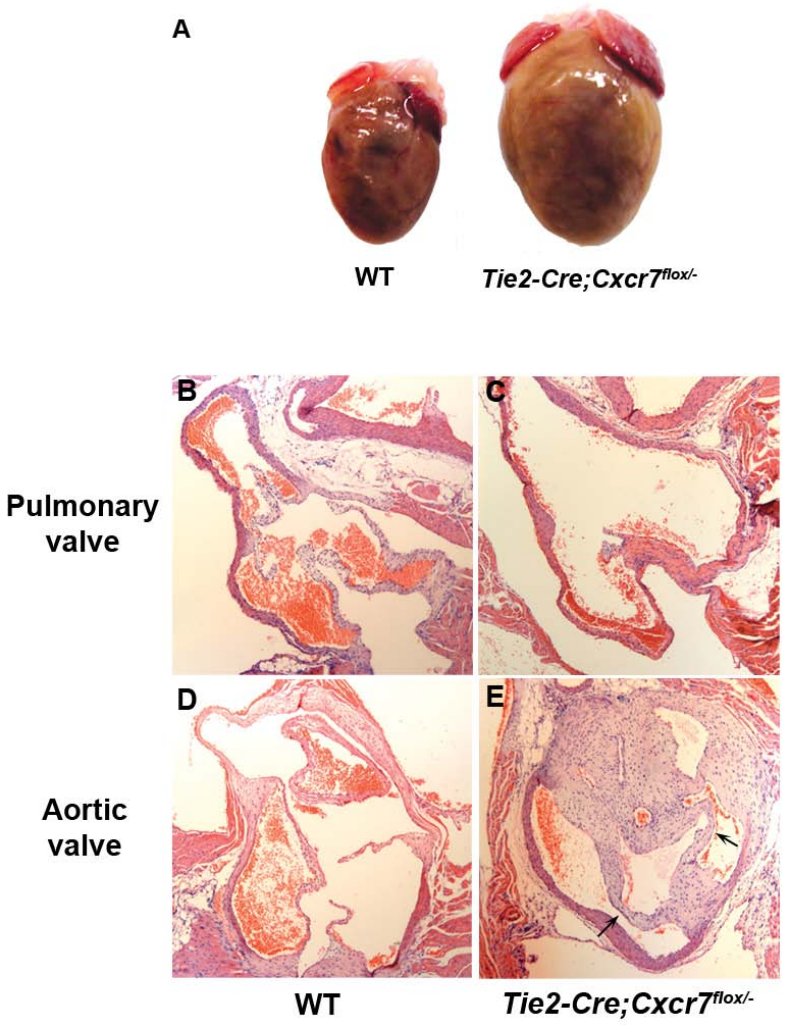

Figure 1. *Tie2-Cre;Cxcr7*$^{flox/-}$ mice have SL valve stenosis. (**A)** Photograph of whole hearts taken from 6-month-old wild-type and *Tie2-Cre;Cxcr7*$^{flox/-}$ mice. Endothelial-specific deletion of *Cxcr7* caused massive hypertrophy. (**B-E)** Heart sections of 6-month-old wild-type and *Tie2-Cre;Cxcr7*$^{flox/-}$ mice were stained with hematoxylin-eosin. *Tie2-Cre;Cxcr7*$^{flox/-}$ mice have SL valve stenosis similar to that in *Cxcr7*$^{-/-}$ mice but a milder pulmonary valve phenotype. Aortic valve leaflets are often fused in mutants (arrows in E).

Figure 2

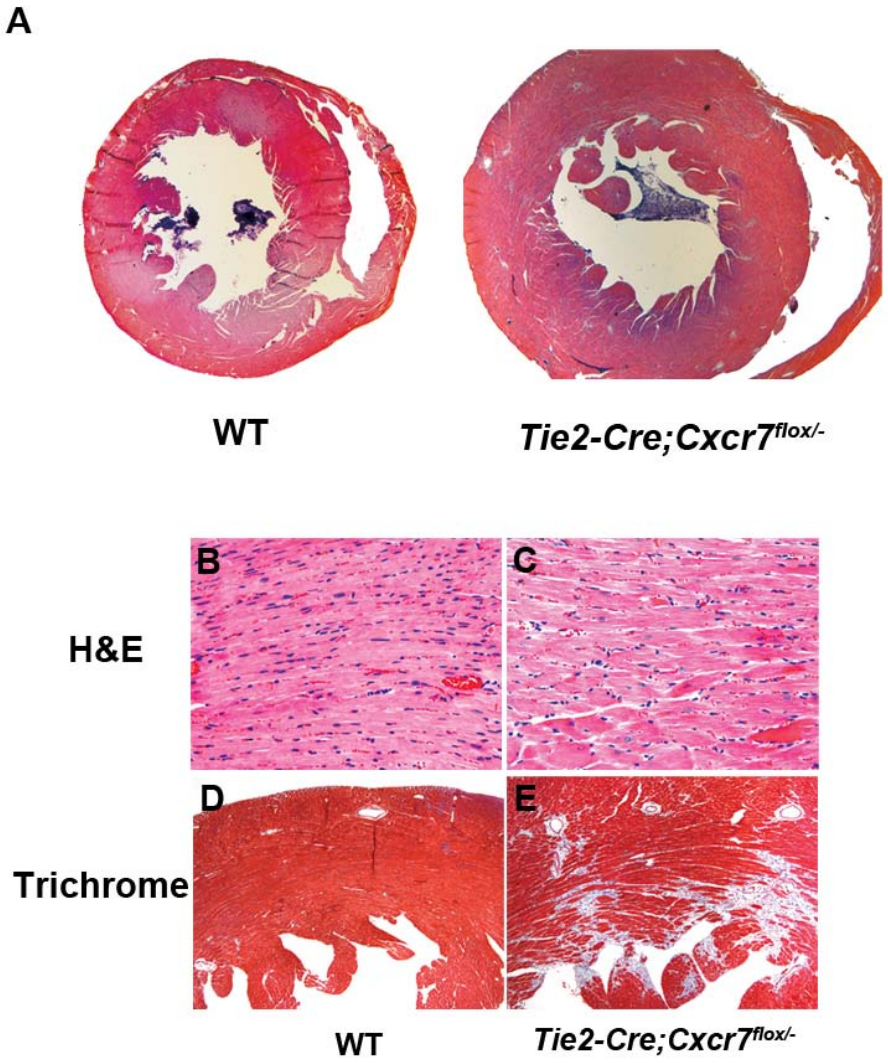

Figure 2. *Tie2-Cre;Cxcr7*$^{flox/-}$ develop cardiac hypertrophy. (A) Transverse sections of wild-type and *Tie2-Cre;Cxcr7*$^{flox/-}$ hearts at 6 months of age. The mutant hearts have a thicker ventricular wall than the wild-type hearts but have similarly sized ventricular cavities. **(B-C)** Magnified images (20x) of the wild-type and *Tie2-Cre;Cxcr7*$^{flox/-}$ heart sections stained with hematoxylin-eosin. Myocardial structure is disarrayed and the size of cardiomyocytes is bigger in the mutant hearts. **(D-E)** Masson's trichrome staining shows more collagen deposition (blue) in the mutant hearts.

Figure 3

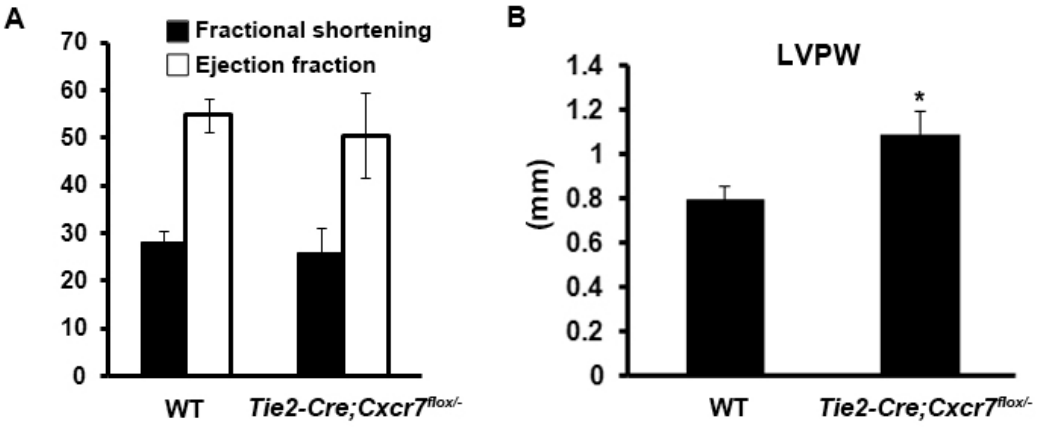

Figure 3. Echocardiographic analysis of *Tie2-Cre;Cxcr7$^{flox/-}$* hearts. (A) Fractional shortening and ejection fraction are similar between wild-type and *Tie2-Cre;Cxcr7$^{flox/-}$* mice at 6 months of age. **(B)** Left ventricular posterior wall (LVPW), measured by echocardiography, is ~1.4-fold thicker in the mutant hearts than in the wild-type hearts (n=3 per group). *P<0.05.

CHAPTER FOUR

CXCR7 MODULATES BONE MORPHOGENETIC PROTEIN SIGNALING TO REGULATE CELL PROLIFERATION IN SEMILUNAR VALVES

Introduction

Endocardial cells that have migrated into cardiac jelly to form ECCs proliferate and secret ECM proteins to produce swellings of the ECCs. Later during the ECC/valve primordia remodeling process, a subset of cushion mesenchymal cells undergo apoptosis to reduce the size of the valves and to form thin leaflets [93]. Cardiac valve hyperplasia can result from increased proliferation, decreased apoptosis, or both of valve mesenchymal cells during valve remodeling.

BMPs promote mesenchymal cell proliferation as well as EMT of endocardial cells in the cardiac cushions. *Bmp4* mouse mutants have hypocellular cardiac cushions [105, 106], and double mutants for *Bmp6/7* and mutants for *Bmpr-II* have hypoplastic OFT cushions with relatively normal AVC cushions [91, 107]. On the other hand, EGF signaling inhibits proliferation of cushion mesenchymal cells through antagonism of BMP-mediated activation of Smad1/5/8 [165-167]. Therefore, mutations causing reduced EGF signaling result in hypercellular endocardial cushions.

Results

Increased Proliferation of SL Valve Mesenchymal Cells in Cxcr7 Knockout Mice

Cxcr7$^{-/-}$ mice had SL valve thickening after E14, implying the defects during valve remodeling. To investigate whether proliferation or apoptosis of SL valve mesenchymal

cells was affected in *Cxcr7*$^{-/-}$ embryos, I analyzed cell proliferation by phospho-histone H3 (pH3) immunofluorescence (Fig. 1A, B) and cell death by TUNEL (terminal deoxynucleotidyl transferase-mediated dUTP nick end labeling) assay (Fig. 1D, E) at various developmental stages. In the wild-type SL valves, the percentage of cells undergoing mitosis decreased as embryos grew older. In contrast, the *Cxcr7*$^{-/-}$ SL valves had ~2-fold more pH3-positive mesenchymal cells than the wild-type valves at E14.0, and 3.5-fold more at E15.5 (Fig. 1C). No difference was detected between pulmonary and aortic valves. The percentages of cells undergoing apoptosis were almost identical in the wild-type and *Cxcr7*$^{-/-}$ SL valves (Fig. 1D, E).

Increased BMP Signaling in SL Valve Mesenchymal Cells in Cxcr7 Knockout Mice

A hypomorphic allele of EGFR also results in thickening of semilunar valves [111], and the mutation of one of its ligands, HB-EGF, leads to dysregulation of BMP signaling and similar valve stenosis in mice [113]. To determine whether BMP signaling is increased in *Cxcr7*$^{-/-}$ SL valves, I performed immunostaining for phospho-Smad1/5/8 (pSmad1/5/8), which transduce BMP signaling. pSmad1/5/8 levels were about 1.5-fold higher in the *Cxcr7*$^{-/-}$ SL valves than in the wild-type valves throughout development (Fig. 2A–E).

Discussion

Hyperplastic ECCs/valve primordia can occur by increased EMT or proliferation of cells in the ECC, or both. Normal cushion sizes in *Cxcr7*$^{-/-}$ mouse embryos until E14 indicate that the valve defects in the *Cxcr7*$^{-/-}$ mice may originate from increased proliferation of

cushion mesenchymal cells. The pH3 immunostaining proves that is the case. Why only the OFT cushions are affected is not clear, but difference between OFT and AVC valve development has been reported. As mentioned in the chapter 1, *Bmp6/7* double mutants and *Bmpr-II* mutants only have OFT cushion defects. Hypomorphic *Egfr* mutation also causes only SL valve hyperplasia but the complete loss of *Egfr* results in both SL and atrioventricular valve defects [111, 113], implying that the SL valve morphogenesis might be more sensitive to perturbations. CXCR7 might affect only a subset of BMP signaling pathways that are predominantly active in the OFT, because BMP ligands and receptors display very dynamic expression patterns during cardiac development, and some of them are more strongly expressed in the OFT than in the AVC, or vice versa [168].

Increased BMP signaling in the OFT cushions of the *Cxcr7*$^{-/-}$ mouse embryos implies that CXCR7 inhibits cushion mesenchymal cell proliferation by suppressing BMP signaling. The direct relationship between CXCR7 and BMP signaling is not known, but CXCR7 might activate EGF signaling to suppress BMP signaling because reduced EGF signaling produces very similar cardiac phenotypes to cardiac defects in the *Cxcr7*$^{-/-}$ mice. Addition of CXCL12 to primary sheep aortic valve mesenchymal cells, which express *Cxcr7*, did not activate EGFR (data not shown). Nevertheless, the link between CXCR7 and EGF signaling cannot be ruled out because there is evidence that unknown CXCR7 ligand(s) exist [140].

Materials and Methods

Immunofluorescent pH3 Staining

Paraffin-embedded embryos of wild-type and *Cxcr7*$^{-/-}$ mice were cut at various stages either transversely or coronally. Sections were deparaffinized with xylene (Sigma) and blocked by 3% normal serum/1% BSA/PBST (0.1% Tween-20 in PBS), then incubated with phospho-histone H3 antibody (Upstate) at 1:100 dilution at RT for 1-2 hrs. For detection, a FITC-conjugated secondary antibody was used at 1:200 dilution at RT for 1hr, and the slides were mounted with Vectashield containing DAPI (Vector Laboratories).

TUNEL Staining

Slides were prepared as described above. In situ cell death detection kit (Roche) was used following manufacturer's manual. Cells undergoing apoptosis was labeled by FITC.

Immunohistochemical Staining of pSmad1/5/8

Slides were prepared as described above. The overall protocol was same as the pH3 staining until secondary antibody incubation. Phospho-Smad1/5/8 antibody (Cell Signaling) was used at 1:100 dilution. For detection, a horseradish peroxidase–conjugated secondary antibody was used at 1:200 dilution, and the sections were stained with the ABC staining system (Vector Laboratories).

Figures

Figure 1

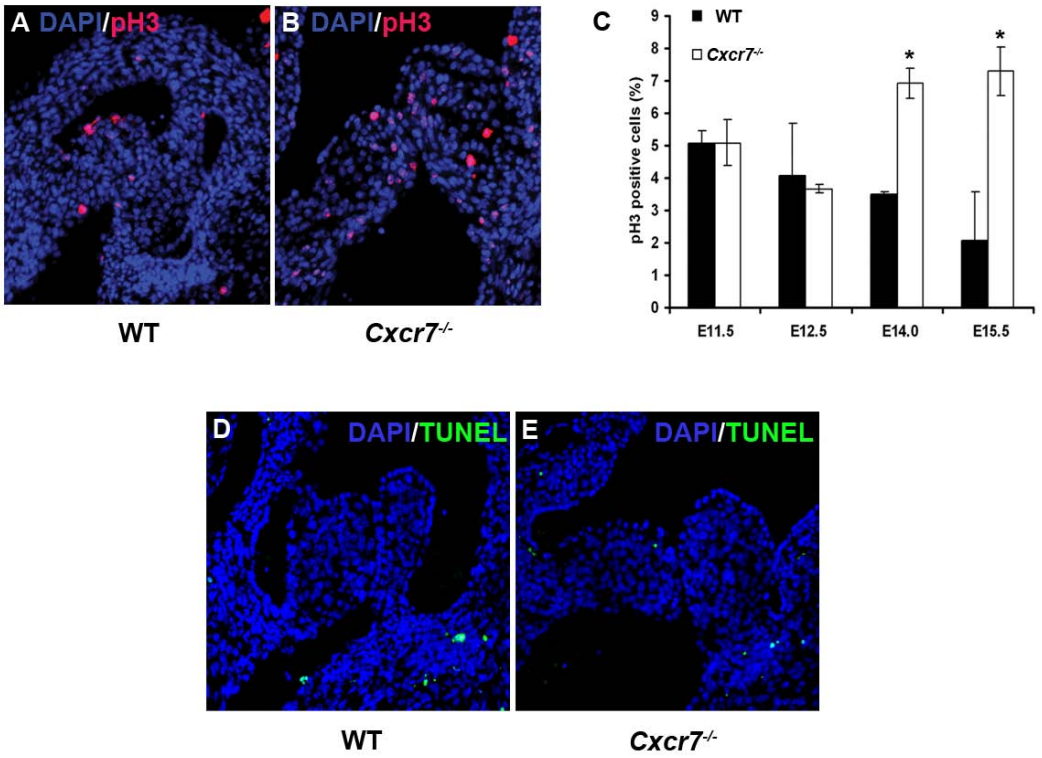

Figure 1. Proliferation of ECC mesenchymal cells is increased in the SL valves. (A-B) Cells undergoing mitosis were stained with phospho-histone H3 antibody (pH3, red) at various embryonic stages. Nuclei were counterstained with DAPI (blue). There are more proliferating cells in the semilunar valves of the *Cxcr7*$^{-/-}$ embryos from E14 onward. Representative sections at E15.5 are shown. **(C)** Quantitative analysis of pH3 immunostaining (pH3-positive cells/total valve cells x 100) showed that the percentage of cells undergoing mitosis in the *Cxcr7*$^{-/-}$ SL valves was increased ~2-fold at E14 and ~3.5-fold at E15.5. *P<0.01. **(D-E)** Cells undergoing apoptosis were analyzed by the TUNEL assay (green). The numbers of apoptotic cells in the OFT endocardial cushions/semilunar valves are similar between the wild-type and *Cxcr7*$^{-/-}$ embryos throughout development. Representative sections at E15.5 are shown.

Figure 2

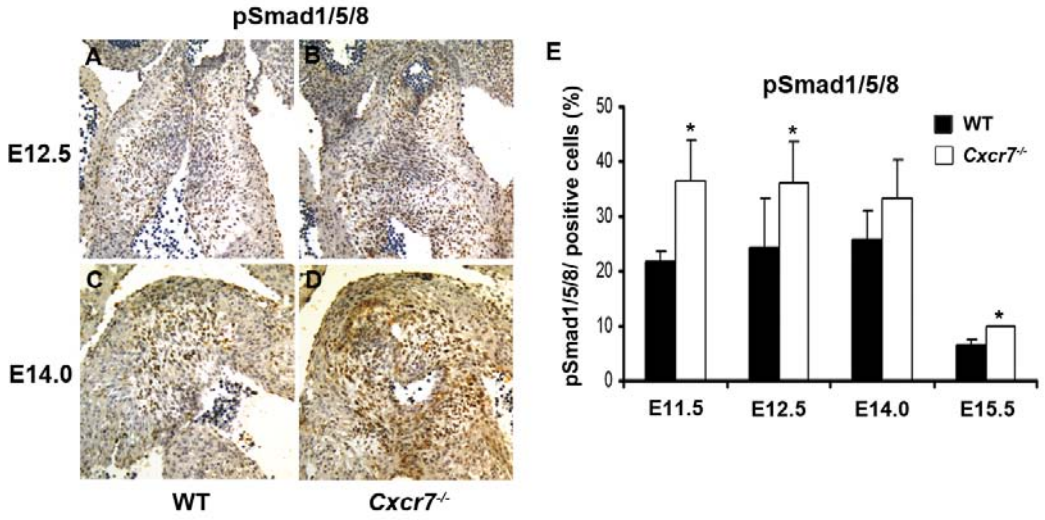

Figure 2. *Cxcr7* deficiency enhances BMP signaling in the OFT endocardial cushions/SL valves. (A-D) Immunohistochemistry with an anti-phospho-Smad1/5/8 (pSmad1/5/8) antibody shows increased BMP signaling in the *Cxcr7*$^{-/-}$ OFT endocardial cushions/SL valves (brown). Nuclei were counterstained with hematoxylin. **(E)** Quantitation of pSmad1/5/8 immunostaining shows that the BMP signaling is increased throughout cardiac valve development in the *Cxcr7*$^{-/-}$ embryos. *P<0.05.

CHAPTER FIVE

CONCLUSIONS AND FUTURE DIRECTIONS

Summary

This study shows that the chemokine receptor CXCR7 is important in cardiac SL valve morphogenesis. *Cxcr7* deletion in mice caused perinatal lethality, likely because of insufficient blood supply to peripheral tissues as a result of severe aortic and pulmonary valve stenosis. Occasional VSD in the membranous ventricular septum and overriding aorta also point toward *Cxcr7* function during ECC morphogenesis, although the possibility of its role in cardiac NCCs cannot be completely ruled out. Loss of *Cxcr7* also increased BMP signaling in SL valves, and caused a sustained high proliferative rate of valve mesenchymal cells during the valve remodeling stage. *Tie2-Cre;Cxcr7*$^{flox/-}$ mice with endothelial cell-specific ablation of *Cxcr7* had similarly enlarged SL valves later in life and developed massive cardiac hypertrophy presumably due to aortic valve stenosis. These mice developed substantial fibrosis in the ventricles and the overall structure of myocardium is disarrayed with enlarged cardiomyocytes. Echocardiogram revealed preserved systolic function with a normally sized ventricular lumen, a concentric hypertrophic phenotype, in the *Tie2-Cre;Cxcr7*$^{flox/-}$ mice.

Possible Link to EGF Signaling

Disruption of EGF signaling pathways in mice causes cardiac valve hypertrophy due to increased proliferation at the late stage of valve development. There is evidence that EGF signaling antagonizes BMP signaling [165-167], and pSmad1/5/8 levels may be increased

in *Hb-egf* knockout valves [113], consistent with a link between EGF signaling and *Cxcr7*. EGFR activation antagonizes BMP signaling by phosphorylating Smad proteins at the linker region that is distinct from phosphorylation sites phosphorylated by BMP receptors [165], or by stabilizing the Smad transcriptional co-repressor TGIF [166]. Both effects are mediated by the MAPK Erk. In one study, *Hb-egf* mRNA was downregulated in *Cxcr7*$^{-/-}$ SL valves, corroborating the relationship between EGF signaling and CXCR7 [152]. When CXCL12/SDF-1 was added to either primary sheep aortic valve mesenchymal cells, which express *Cxcr7*, or to *Cxcr7*-transfected COS1 cells to test whether CXCR7 acts as a positive upstream regulator of EGF signaling, EGFR activation was not observed. This result may indicate that (1) there is no interaction between CXCR7 and EGF signaling, (2) proper extracellular environment, such as cardiac cushion ECM, is required for their interaction because *in vitro* experiment lacked ECM environment, or (3) CXCL12 is not the ligand required for CXCR7 function during valve development. A study in B cells showed that unknown ligand(s) distinct from CXCL12 and CXCL11 exist, even though its identity or expression pattern is not known [140]. Although *Cxcr7* deficiency and disruption of EGF signaling cause similar SL valve phenotypes, VSD and overriding aorta are unique to *Cxcr7*$^{-/-}$ mice, suggesting that CXCR7 activates or inhibits additional pathways.

Other *Cxcr7* Knockout Studies

While I was working on this project, two separate groups reported their findings from *Cxcr7* knockout studies. Results of this study are consistent with the first report of *Cxcr7* knockout phenotypes [152] but not with a subsequent independent *Cxcr7* knockout study

[169]. Perinatal lethality was observed in both studies. However, Gerrits et al. did not observe SL valve thickening or VSDs and concluded that the enlarged hearts in *Cxcr7*-null mice were due to hyperplasia, not hypertrophy. In contrast, Sierro et al. observed aortic and pulmonary valve thickening, as well as bicuspid aortic valves, a finding I did not observe even though occasional aortic valve fusions at their bases were observed. These discrepancies might reflect differences in genetic background, knockout strategies, or effects on neighboring genes. Gerrits et al. knocked in the *β-galactosidase* (*LacZ*) transgene in the place of *Cxcr7* exon2, while this study and Sierro et al. replaced the exon2 with a *loxP*-flanked conditional allele. No predicted microRNAs are in this locus, making it less likely that there are differences in the deletion of potentially embedded genes.

Mechanisms of CXCR7 Signaling

In spite of sharing the same ligand, CXCL12, *Cxcr7* and *Cxcr4* knockout mice have different cardiac phenotypes. VSD is the major cardiac phenotype in *Cxcr4* and *Cxcl12* knockout mice, but those mice have intact SL valves [132-135]. These differences might suggest either (1) CXCR7 is a silent receptor that does not activate any downstream signaling upon ligand binding, or (2) function of CXCR7 in the heart is independent of the CXCR4-CXCL12 axis. However, recent findings suggest the connection between CXCR7 and CXCR4 [137, 139, 146, 149, 150, 152, 153, 170]. The interaction between CXCR7 and CXCR4 are largely two folds: (1) CXCL12 sequestration by CXCR7 to regulate the extracellular CXCL12 level available to CXCR4, or (2) heterodimerization between CXCR7 and CXCR4. Since the studies that reported heterodimerization used

different methods and cell types, some studies showed positive interactions while others showed negative interactions. Nonetheless, it seems like CXCR7 binding to CXCR4 induces conformational changes in CXCR4 and affects its coupling property to downstream G proteins.

Although binding of CXCL12 or CXCL11 to CXCR7 does not activate classical chemokine pathways such as Ca^{2+} mobilization or MAPK signaling, one study showed that a synthetic CXCR7 ligand can elicit Ca^{2+} response and Gi-coupled signaling, implying that CXCR7 actually retains the ability to transduce downstream signaling [171]. It is not known whether this activity is physiologically relevant, but the evidence of CXCR4- or CXCL12-independent CXCR7 functions and the existence of unknown ligands for CXCR7 suggest the presence of yet undiscovered mechanisms of CXCR7 [131, 143, 147]. Moreover, constant interaction of CXCR7 with Gi signaling components in resting state seems to prime CXCR7 for instant activation upon ligand binding [149, 151, 153].

Future Directions

CXCR7 has been implicated in many physiological and pathological processes without knowing its exact mechanisms. Consequently, the interpretation of results varied immensely and sometimes contradicted each other. Therefore, dissecting its mechanism is of utmost importance considering CXCR7's implication in tumor biology and cardiac valve morphogenesis. A large scale screen would be necessary to identify additional CXCR7 ligands other than CXCL11 and CXCL12. Discovery of new ligand(s) for CXCR7 may explain why CXCR7 knockout mice share the VSD phenotype but not SL

valve stenosis with CXCR4 or CXCL12 knockout mice, and also may help elucidate the downstream pathways of CXCR7.

The interaction between CXCR7 and EGF signaling, and between CXCR7 and CXCR4 could be tested genetically. First, it would be interesting to see whether overexpression of EGF signaling components can rescue *Cxcr7* null phenotypes. Also, by using OFT cushion explant taken from *Cxcr7*$^{-/-}$ heart, the interaction between CXCR7 and EGF signaling can be tested *in vitro*. For example, HB-EGF can be added to the media to test whether the proliferation defect of the *Cxcr7*$^{-/-}$ cushion explant can be rescued by activation of EGF signaling. As for the interaction with CXCR4, *Cxcr4/7* double mutations would help explain their genetic relationship by observing whether the compound mutation rescues or exacerbates the phenotype. One obstacle for this approach would be that they reside on the same chromosome, chromosome 1 in mouse, which lowers the recombination frequency between two genes and consequently makes it difficult to obtain the compound mutants.

Finally, milder phenotype of *Tie2-Cre;Cxcr7*$^{flox/-}$ mice than *Cxcr7*$^{-/-}$ mice implies function of *Cxcr7* in cell types other than endothelial derivatives. This can be tested by using cell type-specific *Cre* lines. Considering the expression pattern of *Cxcr7* during early mouse development and cardiac phenotypes like VSDs and overriding aorta, cardiomyocytes-specific *Cre* mice, such as *α-myosin heavy chain-Cre* mice, or NCC-specific *Cre* mice, such as *Wnt1-Cre* mice, could be useful.

Conclusions and Perspectives

Valve defects are among the most common forms of human congenital heart disease and typically involve abnormal thickening of the aortic or pulmonary valves. The consequences can range from neonatal cardiac failure to cardiac hypertrophy later in life, depending on the severity of the stenosis. Numerous signaling pathways have been linked to valve formation, and disruption of any of these pathways during pregnancy could lead to fatal conditions, underscoring the importance of elucidating the exact mechanisms of valve formation. For instance, the absence of *Ptpn11,* which is involved in a signaling pathway mediated by EGFR, results in dysplastic outflow valves [111]. In humans, mutations of *Ptpn11* cause Noonan syndrome, characterized by pulmonic valve stenosis [75]. Similarly, human mutations in *Notch1* cause thickened aortic valve leaflets and can result in aortic valve stenosis early or later in life [97]. It will be interesting to determine whether CXCR7 or pathways that it regulates also contribute to human aortic or pulmonary valve disease. If so, understanding the mechanism of CXCR7 in the heart could contribute to better diagnosis, treatment, and prevention of cardiac valve defects in humans.

APPENDIX A

GENERATION OF TARGETED *CXCR7* CONDITIONAL ALLELE

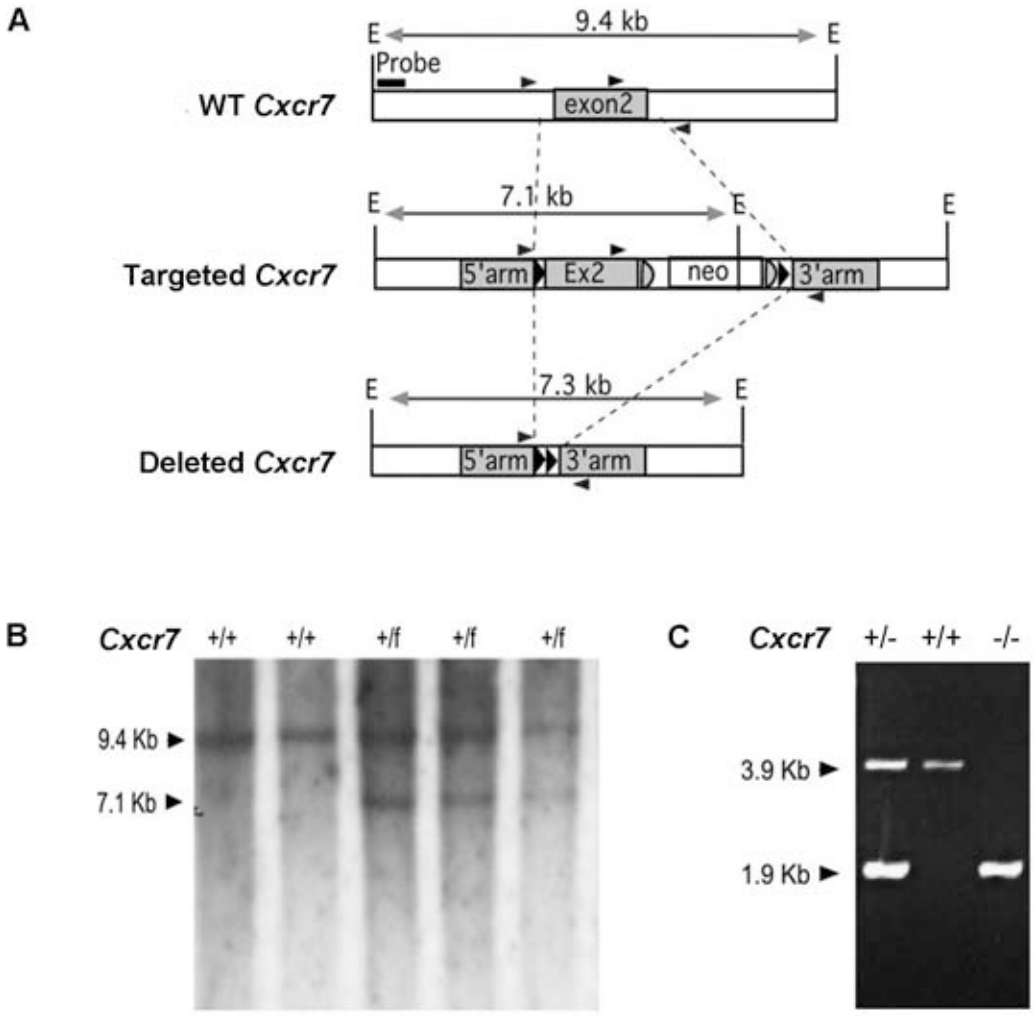

(A) Schematic representation of the wild-type *Cxcr7* locus, the targeted allele, and the deleted locus. Shaded regions represent exon 2 (exon 2, top); the cloning fragment which includes exon 2 and about 100 bp up- and downstream of exon 2 (Ex2, middle); the 5' homologous arm, which was cloned from DNA immediately upstream of exon 2 (5' arm, middle and lower); and the 3' homologous arm, which was cloned from DNA immediately downstream of exon 2 (3' arm, middle and lower). Black triangles indicate *LoxP* sites; arrowhead indicates primer sites used for genotyping. E, EcoRV; neo, neomycin-resistance gene cassette. **(B)** Southern blot analysis of ES cell clones showing non-targeted (+/+) and targeted (+/f) clones. The 9.4-kb wild-type and 7.1-kb targeted allele fragments digested with EcoRV were identified with an upstream probe, as shown in (A). **(C)** PCR analysis of genomic DNA from E16.5 wild-type (+/+) embryos or embryos heterozygous (+/–) or homozygous (–/–) for Cre-mediated deletion of the targeted locus. The 3.9-kb wild-type and 1.9-kb deleted products were from a single set of primers outside of exon 2, as shown in (A). (Crawford, D., University of Minnesota, MN).

Materials and Methods

A conditional knockout targeting vector was designed to insert *loxP* sequences about 100–200 base pairs from either side of exon 2 of the *Cxcr7* locus. The targeting vector included a neomycin-resistance gene cassette (neo) downstream of exon 2 and flanked by FRT sites for deletion of neo from the targeted locus if necessary.

Three segments were cloned by PCR from 129/SvEv genomic DNA and inserted into the *pK11-2xLox-MCS12* cloning vector [172]. This vector was kindly provided by Dr. Martin, G. (University of California, San Francisco, CA) and Dr. Koob, M. (University of Minnesota, MN). Fragment Ex2, 10029-12169 (numbered from the start of *Cxcr7* exon 1), include exon 2 plus flanking 100-200bp segments and was inserted into the cloning vector at XhoI and SalI restriction sites, between two loxP sites and 5' to the FRT-flanked neo. 5' arm, 8722-10034, was a 1.3kb fragment cloned from DNA immediately upstream of Ex2 and inserted into the cloning vector at XbaI and NheI sites. 3' arm, 12170-14468, was a 2.3kb fragment cloned from DNA immediately downstream of Ex2

and inserted into the cloning vector at ApaI and NotI sites. Thymidine kinase (TK) gene cassette was cloned from the *pKO-Scrambler* cloning vector and inserted into the far outside of the 3' arm for negative selection. Primers used for cloning of genomic regions were: (1) Ex2: 5' – GTAC CTCGAGCCCAGCACCATGTAACCTTAGG, 3' – GTAC GTCGACGCTTTCAAACCCAAAGCACACAT; 5' arm: 5' – GTAC GCTAGCAGT GGGGCTGGGCTTTCCTAA, 3' – GTAC TCTAGACTGGGGAGGGGCTGTG TTTGT; and 3' arm: 5' – GATC GGGCCCATGTTTGGGCTTTGGATGG, 3' – GATC GCGGCCGCCCTGGGCCTCTGGAGTCTA.

The linearized targeting vector was electroporated into 129/SvEv embryonic stem cells (Dr. Koller, B., University of North Carolina, Chapel Hill, NC). ES clones were screened by PCR and verified by Southern blot. The template for the probe was amplified from 129/SvEv genomic DNA, upstream and outside the cloned homologous region, using the primers: 5' – GTACGGTTCTCTGCCCCTGGACTGTG, and 3' – GTACGCACGCCTAGCCTGGAAATG. Correctly targeted ES cells were injected into C57BL/6 mouse blastocysts. Chimeric offspring were crossed with C57BL/6 mice, and agouti offspring were screened for the targeted allele, $Cxcr7^{flox}$. Primers used to detect the targeted versus wild-type alleles were: 5' – GGGCGGC TGGGTCCTGTGGTTTCT, 3' – GGGGAAGACGGCAGGCAGATG TTTGTTA. $Cxcr7^{flox}$ mice were crossed with *deleter Cre* transgenic mice to generate $Cxcr7^{+/-}$. *Deleter Cre* mice were kindly provided by Dr. K. Rajewsky (Harvard Medical School, Boston, MA, with permission from the University of Cologne, Cologne, Germany) [160].

APPENDIX B

CALCIUM DEPOSITION OF *TIE2-CRE;CXCR7$^{FLOX/-}$* AORTIC VALVES

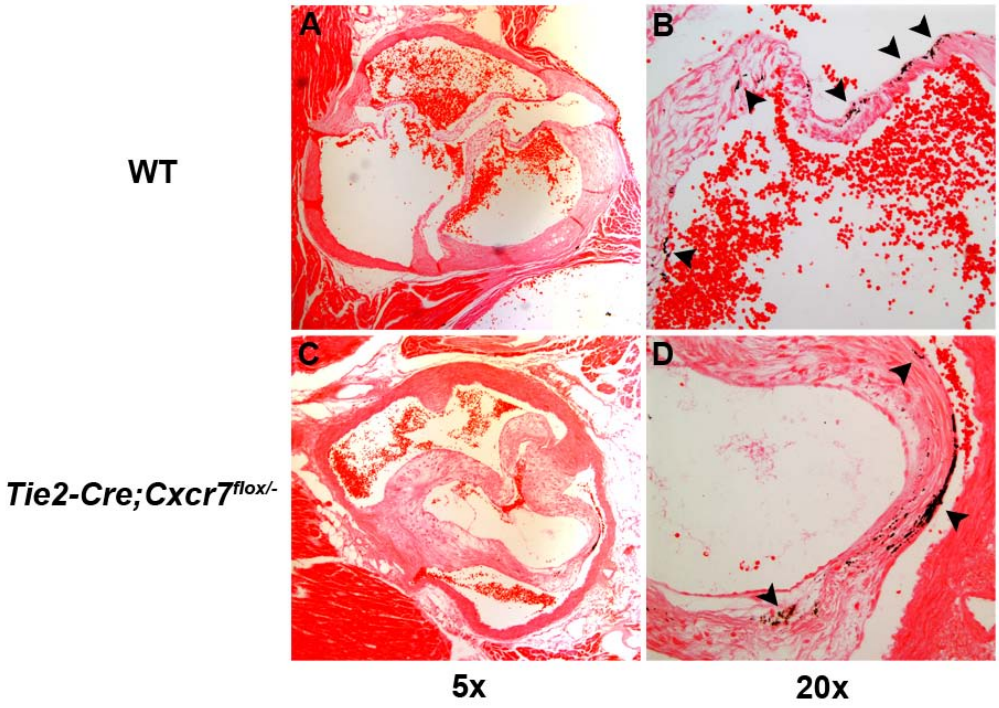

(A-D) The amount calcium deposition (black) in the aortic valves of *Tie2-Cre;Cxcr7$^{flox/-}$* mice was measured by Von Kossa staining at 6 months of age. The amount of calcium in the aortic valves was similar between wild-type and *Tie2-Cre;Cxcr7$^{flox/-}$* mice. Tissues were counterstained with nuclear fast red (red and pink). B and D are high magnification images of A and C, respectively, and show the area where calcium accumulation could be seen (arrow heads).

Materials and Methods

Paraffin sections were made from 6-month-old wild-type and *Tie2-Cre;Cxcr7$^{flox/-}$* hearts.

After sections were deparaffinized, they were incubated with 1% silver nitrate solution in

a clear glass coplin jar placed under ultraviolet light for 20 minutes and washed with

distilled water. Sections were treated with 5% sodium thiosulfate for 5 min to remove unreacted silver and counterstained with nuclear fast red for 5 min. Sections were dehydrated through graded alcohol and cleared in xylene.

APPENDIX C

ECHOCARDIOGRAPHIC ANALYSIS OF *TIE2-CRE;CXCR7$^{FLOX/-}$* MICE

< Wild-type >

		AV peak velocity (mm/s)	PV peak velocity (mm/s)	Fractional shortening (%)	Ejection fraction (%)	LVPW-d (mm)	LVPW-s (mm)	IVS-d (mm)	IVS-s (mm)	LVID-d (mm)	LVID-s (mm)
ID	Mode → Trial ↓	PW Doppler	PW Doppler			M-Mode	M-Mode	M-Mode	M-Mode	M-Mode	M-Mode
WT 1	1	930.14	701.14	30.77	59.00	0.79	1.07	0.74	1.15	3.91	2.71
	2		924.21	30.95	59.74	1.04	1.04	0.96	1.31	3.45	2.38
	3			27.78	54.47	0.66	1.04	0.88	1.12	3.94	2.84
	Ave	930.14	812.68	29.83	57.74	0.83	1.05	0.86	1.19	3.77	2.64
WT 2	1	1807.29	968.17	27.10	53.16	0.95	1.23	1.27	1.58	4.23	3.09
	2		844.53	31.71	59.86	0.87	0.96	0.84	1.41	5.08	3.73
	3			27.97	54.22	0.68	0.93	0.93	1.29	4.60	3.31
	Ave	1807.29	906.35	28.93	55.75	0.83	1.04	1.01	1.43	4.64	3.38
WT 3	1	821.16	636.39	25.00	49.87	0.79	1.07	0.77	1.07	4.16	3.12
	2			25.19	49.90	0.70	0.80	0.70	1.07	4.50	3.37
	3			26.77	52.64	0.70	0.87	0.87	1.00	4.23	3.10
	Ave	821.16	636.39	25.65	50.80	0.73	0.91	0.78	1.05	4.30	3.20
	Ave	1186.20	785.14	28.14	54.76	0.80	1.00	0.88	1.22	4.23	3.07
	SD	540.64	137.07	2.20	3.57	0.06	0.08	0.12	0.19	0.44	0.38

< *Tie2-Cre;Cxcr7$^{flox/-}$* >

		AV peak velocity (mm/s)	PV peak velocity (mm/s)	Fractional shortening (%)	Ejection fraction (%)	LVPW-d (mm)	LVPW-s (mm)	IVS-d (mm)	IVS-s (mm)	LVID-d (mm)	LVID-s (mm)
ID	Mode → Trial ↓	PW Doppler	PW Doppler			M-Mode	M-Mode	M-Mode	M-Mode	M-Mode	M-Mode
KO 1	1	864.43	743.35	28.12	54.81	1.23	1.66	1.20	1.72	4.16	2.99
	2	1148.37		33.61	62.99	1.14	1.79	1.30	1.75	3.96	2.63
	3			29.91	57.66	1.20	1.75	1.49	1.95	3.93	2.53
	Ave	1006.40	743.35	30.55	58.49	1.19	1.73	1.33	1.81	4.02	2.72
KO 2	1	2762.77	1036.41	19.50	40.33	0.98	1.23	0.98	1.26	4.35	3.50
	2	1572.32		30.38	58.07	1.01	1.29	0.96	1.34	4.32	3.01
	3			30.41	58.12	0.93	1.13	0.84	1.31	4.30	2.99
	Ave	2167.55	1036.41	26.76	52.17	0.97	1.22	0.93	1.30	4.32	3.17
KO 3	1	1879.88	834.26	21.83	43.91	0.79	0.97	0.79	1.08	5.10	3.98
	2			14.39	30.80	1.21	1.24	1.11	1.18	4.44	3.80
	3			23.66	47.47	1.28	1.68	0.91	1.38	4.41	3.36
	Ave	1879.88	834.26	19.96	40.73	1.09	1.30	0.94	1.21	4.65	3.71
	Ave	1684.61	871.34	25.76	50.46	1.09	1.42	1.06	1.44	4.33	3.20
	SD	604.70	150.01	5.36	9.00	0.11	0.28	0.23	0.32	0.32	0.50
	P value	0.35	0.50	0.52	0.48	**0.02**	0.07	0.29	0.37	0.77	0.74

AV, aortic valve; PV, pulmonary valve; LVPW-d/s, left ventricular posterior wall-diastolic/systolic; IVS-d/s, interventricular septum-diastolic/systolic; LVID-d/s, left ventricular internal dimension-diastolic/systolic; WT, wild-type; Ave, average; KO, knockout.

BIBLIOGRAPHY

1. Srivastava, D. (2006). Making or breaking the heart: from lineage determination to morphogenesis. Cell *126*, 1037-1048.

2. Nemer, M. (2008). Genetic insights into normal and abnormal heart development. Cardiovasc Pathol *17*, 48-54.

3. Lloyd-Jones, D., Adams, R., Carnethon, M., De Simone, G., Ferguson, T.B., Flegal, K., Ford, E., Furie, K., Go, A., Greenlund, K., et al. (2009). Heart disease and stroke statistics--2009 update: a report from the American Heart Association Statistics Committee and Stroke Statistics Subcommittee. Circulation *119*, e21-181.

4. Srivastava, D. (2006). Genetic regulation of cardiogenesis and congenital heart disease. Annu Rev Pathol *1*, 199-213.

5. Bruneau, B.G. (2008). The developmental genetics of congenital heart disease. Nature *451*, 943-948.

6. Buckingham, M., Meilhac, S., and Zaffran, S. (2005). Building the mammalian heart from two sources of myocardial cells. Nat Rev Genet *6*, 826-835.

7. Mjaatvedt, C.H., Nakaoka, T., Moreno-Rodriguez, R., Norris, R.A., Kern, M.J., Eisenberg, C.A., Turner, D., and Markwald, R.R. (2001). The outflow tract of the heart is recruited from a novel heart-forming field. Dev Biol *238*, 97-109.

8. Waldo, K.L., Kumiski, D.H., Wallis, K.T., Stadt, H.A., Hutson, M.R., Platt, D.H., and Kirby, M.L. (2001). Conotruncal myocardium arises from a secondary heart field. Development *128*, 3179-3188.

9. Kelly, R.G., Brown, N.A., and Buckingham, M.E. (2001). The arterial pole of the mouse heart forms from Fgf10-expressing cells in pharyngeal mesoderm. Dev Cell *1*, 435-440.

10. Zaffran, S., Kelly, R.G., Meilhac, S.M., Buckingham, M.E., and Brown, N.A. (2004). Right ventricular myocardium derives from the anterior heart field. Circulation research *95*, 261-268.

11. Cai, C.L., Liang, X., Shi, Y., Chu, P.H., Pfaff, S.L., Chen, J., and Evans, S. (2003). Isl1 identifies a cardiac progenitor population that proliferates prior to differentiation and contributes a majority of cells to the heart. Dev Cell *5*, 877-889.

12. Meilhac, S.M., Esner, M., Kelly, R.G., Nicolas, J.F., and Buckingham, M.E. (2004). The clonal origin of myocardial cells in different regions of the embryonic mouse heart. Dev Cell *6*, 685-698.

13. Christoffels, V.M., Habets, P.E., Franco, D., Campione, M., de Jong, F., Lamers, W.H., Bao, Z.Z., Palmer, S., Biben, C., Harvey, R.P., et al. (2000). Chamber formation and morphogenesis in the developing mammalian heart. Dev Biol *223*, 266-278.

14. Christoffels, V.M., Hoogaars, W.M., Tessari, A., Clout, D.E., Moorman, A.F., and Campione, M. (2004). T-box transcription factor Tbx2 represses differentiation and formation of the cardiac chambers. Dev Dyn *229*, 763-770.

15. Hove, J.R., Koster, R.W., Forouhar, A.S., Acevedo-Bolton, G., Fraser, S.E., and Gharib, M. (2003). Intracardiac fluid forces are an essential epigenetic factor for embryonic cardiogenesis. Nature *421*, 172-177.

16. Olson, E.N., and Schneider, M.D. (2003). Sizing up the heart: development redux in disease. Genes Dev *17*, 1937-1956.

17. Kastner, P., Messaddeq, N., Mark, M., Wendling, O., Grondona, J.M., Ward, S., Ghyselinck, N., and Chambon, P. (1997). Vitamin A deficiency and mutations of RXRalpha, RXRbeta and RARalpha lead to early differentiation of embryonic ventricular cardiomyocytes. Development *124*, 4749-4758.

18. Sucov, H.M., Dyson, E., Gumeringer, C.L., Price, J., Chien, K.R., and Evans, R.M. (1994). RXR alpha mutant mice establish a genetic basis for vitamin A signaling in heart morphogenesis. Genes Dev *8*, 1007-1018.

19. Gassmann, M., Casagranda, F., Orioli, D., Simon, H., Lai, C., Klein, R., and Lemke, G. (1995). Aberrant neural and cardiac development in mice lacking the ErbB4 neuregulin receptor. Nature *378*, 390-394.

20. Lee, K.F., Simon, H., Chen, H., Bates, B., Hung, M.C., and Hauser, C. (1995). Requirement for neuregulin receptor erbB2 in neural and cardiac development. Nature *378*, 394-398.

21. Zhao, Y.Y., Sawyer, D.R., Baliga, R.R., Opel, D.J., Han, X., Marchionni, M.A., and Kelly, R.A. (1998). Neuregulins promote survival and growth of cardiac myocytes. Persistence of ErbB2 and ErbB4 expression in neonatal and adult ventricular myocytes. J Biol Chem *273*, 10261-10269.

22. Pereira, F.A., Qiu, Y., Zhou, G., Tsai, M.J., and Tsai, S.Y. (1999). The orphan nuclear receptor COUP-TFII is required for angiogenesis and heart development. Genes Dev *13*, 1037-1049.

23. Hyer, J., Johansen, M., Prasad, A., Wessels, A., Kirby, M.L., Gourdie, R.G., and Mikawa, T. (1999). Induction of Purkinje fiber differentiation by coronary arterialization. Proc Natl Acad Sci U S A *96*, 13214-13218.

24. Stoller, J.Z., and Epstein, J.A. (2005). Cardiac neural crest. Seminars in cell & developmental biology *16*, 704-715.

25. Zaffran, S., and Frasch, M. (2002). Early signals in cardiac development. Circulation research *91*, 457-469.

26. Brand, T. (2003). Heart development: molecular insights into cardiac specification and early morphogenesis. Dev Biol *258*, 1-19.

27. Lyons, I., Parsons, L.M., Hartley, L., Li, R., Andrews, J.E., Robb, L., and Harvey, R.P. (1995). Myogenic and morphogenetic defects in the heart tubes of murine embryos lacking the homeo box gene Nkx2-5. Genes Dev *9*, 1654-1666.

28. Tanaka, M., Wechsler, S.B., Lee, I.W., Yamasaki, N., Lawitts, J.A., and Izumo, S. (1999). Complex modular cis-acting elements regulate expression of the cardiac specifying homeobox gene Csx/Nkx2.5. Development *126*, 1439-1450.

29. Biben, C., and Harvey, R.P. (1997). Homeodomain factor Nkx2-5 controls left/right asymmetric expression of bHLH gene eHand during murine heart development. Genes Dev *11*, 1357-1369.

30. Yamagishi, H., Yamagishi, C., Nakagawa, O., Harvey, R.P., Olson, E.N., and Srivastava, D. (2001). The combinatorial activities of Nkx2.5 and dHAND are essential for cardiac ventricle formation. Dev Biol *239*, 190-203.

31. Firulli, A.B., McFadden, D.G., Lin, Q., Srivastava, D., and Olson, E.N. (1998). Heart and extra-embryonic mesodermal defects in mouse embryos lacking the bHLH transcription factor Hand1. Nature genetics *18*, 266-270.

32. McFadden, D.G., Barbosa, A.C., Richardson, J.A., Schneider, M.D., Srivastava, D., and Olson, E.N. (2005). The Hand1 and Hand2 transcription factors regulate expansion of the embryonic cardiac ventricles in a gene dosage-dependent manner. Development *132*, 189-201.

33. Riley, P., Anson-Cartwright, L., and Cross, J.C. (1998). The Hand1 bHLH transcription factor is essential for placentation and cardiac morphogenesis. Nature genetics *18*, 271-275.

34. Srivastava, D., Thomas, T., Lin, Q., Kirby, M.L., Brown, D., and Olson, E.N. (1997). Regulation of cardiac mesodermal and neural crest development by the bHLH transcription factor, dHAND. Nature genetics *16*, 154-160.

35. Thomas, T., Kurihara, H., Yamagishi, H., Kurihara, Y., Yazaki, Y., Olson, E.N., and Srivastava, D. (1998). A signaling cascade involving endothelin-1, dHAND and msx1 regulates development of neural-crest-derived branchial arch mesenchyme. Development *125*, 3005-3014.

36. Benson, D.W., Silberbach, G.M., Kavanaugh-McHugh, A., Cottrill, C., Zhang, Y., Riggs, S., Smalls, O., Johnson, M.C., Watson, M.S., Seidman, J.G., et al. (1999). Mutations in the cardiac transcription factor NKX2.5 affect diverse cardiac developmental pathways. J Clin Invest *104*, 1567-1573.

37. Schott, J.J., Benson, D.W., Basson, C.T., Pease, W., Silberbach, G.M., Moak, J.P., Maron, B.J., Seidman, C.E., and Seidman, J.G. (1998). Congenital heart disease caused by mutations in the transcription factor NKX2-5. Science *281*, 108-111.

38. Molkentin, J.D. (2000). The zinc finger-containing transcription factors GATA-4, -5, and -6. Ubiquitously expressed regulators of tissue-specific gene expression. J Biol Chem *275*, 38949-38952.

39. Jiang, Y., Tarzami, S., Burch, J.B., and Evans, T. (1998). Common role for each of the cGATA-4/5/6 genes in the regulation of cardiac morphogenesis. Dev Genet *22*, 263-277.

40. Kuo, C.T., Morrisey, E.E., Anandappa, R., Sigrist, K., Lu, M.M., Parmacek, M.S., Soudais, C., and Leiden, J.M. (1997). GATA4 transcription factor is required for ventral morphogenesis and heart tube formation. Genes Dev *11*, 1048-1060.

41. Molkentin, J.D., Lin, Q., Duncan, S.A., and Olson, E.N. (1997). Requirement of the transcription factor GATA4 for heart tube formation and ventral morphogenesis. Genes Dev *11*, 1061-1072.

42. Reiter, J.F., Alexander, J., Rodaway, A., Yelon, D., Patient, R., Holder, N., and Stainier, D.Y. (1999). Gata5 is required for the development of the heart and endoderm in zebrafish. Genes Dev *13*, 2983-2995.

43. Garg, V., Kathiriya, I.S., Barnes, R., Schluterman, M.K., King, I.N., Butler, C.A., Rothrock, C.R., Eapen, R.S., Hirayama-Yamada, K., Joo, K., et al. (2003). GATA4 mutations cause human congenital heart defects and reveal an interaction with TBX5. Nature *424*, 443-447.

44. Bruneau, B.G., Logan, M., Davis, N., Levi, T., Tabin, C.J., Seidman, J.G., and Seidman, C.E. (1999). Chamber-specific cardiac expression of Tbx5 and heart defects in Holt-Oram syndrome. Dev Biol *211*, 100-108.

45. Chapman, D.L., Garvey, N., Hancock, S., Alexiou, M., Agulnik, S.I., Gibson-Brown, J.J., Cebra-Thomas, J., Bollag, R.J., Silver, L.M., and Papaioannou, V.E. (1996). Expression of the T-box family genes, Tbx1-Tbx5, during early mouse development. Dev Dyn *206*, 379-390.

46. Horb, M.E., and Thomsen, G.H. (1999). Tbx5 is essential for heart development. Development *126*, 1739-1751.

47. Bruneau, B.G., Nemer, G., Schmitt, J.P., Charron, F., Robitaille, L., Caron, S., Conner, D.A., Gessler, M., Nemer, M., Seidman, C.E., et al. (2001). A murine model of Holt-Oram syndrome defines roles of the T-box transcription factor Tbx5 in cardiogenesis and disease. Cell *106*, 709-721.

48. Takeuchi, J.K., Ohgi, M., Koshiba-Takeuchi, K., Shiratori, H., Sakaki, I., Ogura, K., Saijoh, Y., and Ogura, T. (2003). Tbx5 specifies the left/right ventricles and ventricular septum position during cardiogenesis. Development *130*, 5953-5964.

49. Basson, C.T., Bachinsky, D.R., Lin, R.C., Levi, T., Elkins, J.A., Soults, J., Grayzel, D., Kroumpouzou, E., Traill, T.A., Leblanc-Straceski, J., et al. (1997). Mutations in human TBX5 [corrected] cause limb and cardiac malformation in Holt-Oram syndrome. Nature genetics *15*, 30-35.

50. Li, Q.Y., Newbury-Ecob, R.A., Terrett, J.A., Wilson, D.I., Curtis, A.R., Yi, C.H., Gebuhr, T., Bullen, P.J., Robson, S.C., Strachan, T., et al. (1997). Holt-Oram syndrome is caused by mutations in TBX5, a member of the Brachyury (T) gene family. Nature genetics *15*, 21-29.

51. Hiroi, Y., Kudoh, S., Monzen, K., Ikeda, Y., Yazaki, Y., Nagai, R., and Komuro, I. (2001). Tbx5 associates with Nkx2-5 and synergistically promotes cardiomyocyte differentiation. Nature genetics *28*, 276-280.

52. Garg, V., Yamagishi, C., Hu, T., Kathiriya, I.S., Yamagishi, H., and Srivastava, D. (2001). Tbx1, a DiGeorge syndrome candidate gene, is regulated by sonic hedgehog during pharyngeal arch development. Dev Biol *235*, 62-73.

53. Jerome, L.A., and Papaioannou, V.E. (2001). DiGeorge syndrome phenotype in mice mutant for the T-box gene, Tbx1. Nature genetics *27*, 286-291.

54. Lindsay, E.A., Vitelli, F., Su, H., Morishima, M., Huynh, T., Pramparo, T., Jurecic, V., Ogunrinu, G., Sutherland, H.F., Scambler, P.J., et al. (2001). Tbx1 haploinsufficieny in the DiGeorge syndrome region causes aortic arch defects in mice. Nature *410*, 97-101.

55. Merscher, S., Funke, B., Epstein, J.A., Heyer, J., Puech, A., Lu, M.M., Xavier, R.J., Demay, M.B., Russell, R.G., Factor, S., et al. (2001). TBX1 is responsible

for cardiovascular defects in velo-cardio-facial/DiGeorge syndrome. Cell *104*, 619-629.

56. Abu-Issa, R., Smyth, G., Smoak, I., Yamamura, K., and Meyers, E.N. (2002). Fgf8 is required for pharyngeal arch and cardiovascular development in the mouse. Development *129*, 4613-4625.

57. Frank, D.U., Fotheringham, L.K., Brewer, J.A., Muglia, L.J., Tristani-Firouzi, M., Capecchi, M.R., and Moon, A.M. (2002). An Fgf8 mouse mutant phenocopies human 22q11 deletion syndrome. Development *129*, 4591-4603.

58. Kochilas, L., Merscher-Gomez, S., Lu, M.M., Potluri, V., Liao, J., Kucherlapati, R., Morrow, B., and Epstein, J.A. (2002). The role of neural crest during cardiac development in a mouse model of DiGeorge syndrome. Dev Biol *251*, 157-166.

59. Vitelli, F., Taddei, I., Morishima, M., Meyers, E.N., Lindsay, E.A., and Baldini, A. (2002). A genetic link between Tbx1 and fibroblast growth factor signaling. Development *129*, 4605-4611.

60. Hu, T., Yamagishi, H., Maeda, J., McAnally, J., Yamagishi, C., and Srivastava, D. (2004). Tbx1 regulates fibroblast growth factors in the anterior heart field through a reinforcing autoregulatory loop involving forkhead transcription factors. Development *131*, 5491-5502.

61. Cai, C.L., Zhou, W., Yang, L., Bu, L., Qyang, Y., Zhang, X., Li, X., Rosenfeld, M.G., Chen, J., and Evans, S. (2005). T-box genes coordinate regional rates of proliferation and regional specification during cardiogenesis. Development *132*, 2475-2487.

62. Singh, M.K., Christoffels, V.M., Dias, J.M., Trowe, M.O., Petry, M., Schuster-Gossler, K., Burger, A., Ericson, J., and Kispert, A. (2005). Tbx20 is essential for cardiac chamber differentiation and repression of Tbx2. Development *132*, 2697-2707.

63. Stennard, F.A., Costa, M.W., Lai, D., Biben, C., Furtado, M.B., Solloway, M.J., McCulley, D.J., Leimena, C., Preis, J.I., Dunwoodie, S.L., et al. (2005). Murine T-box transcription factor Tbx20 acts as a repressor during heart development, and is essential for adult heart integrity, function and adaptation. Development *132*, 2451-2462.

64. Takeuchi, J.K., Mileikovskaia, M., Koshiba-Takeuchi, K., Heidt, A.B., Mori, A.D., Arruda, E.P., Gertsenstein, M., Georges, R., Davidson, L., Mo, R., et al. (2005). Tbx20 dose-dependently regulates transcription factor networks required for mouse heart and motoneuron development. Development *132*, 2463-2474.

65. Harrelson, Z., Kelly, R.G., Goldin, S.N., Gibson-Brown, J.J., Bollag, R.J., Silver, L.M., and Papaioannou, V.E. (2004). Tbx2 is essential for patterning the atrioventricular canal and for morphogenesis of the outflow tract during heart development. Development *131*, 5041-5052.

66. Dodou, E., Verzi, M.P., Anderson, J.P., Xu, S.M., and Black, B.L. (2004). Mef2c is a direct transcriptional target of ISL1 and GATA factors in the anterior heart field during mouse embryonic development. Development *131*, 3931-3942.

67. Laugwitz, K.L., Moretti, A., Lam, J., Gruber, P., Chen, Y., Woodard, S., Lin, L.Z., Cai, C.L., Lu, M.M., Reth, M., et al. (2005). Postnatal isl1+ cardioblasts enter fully differentiated cardiomyocyte lineages. Nature *433*, 647-653.

68. Lin, Q., Schwarz, J., Bucana, C., and Olson, E.N. (1997). Control of mouse cardiac morphogenesis and myogenesis by transcription factor MEF2C. Science *276*, 1404-1407.

69. von Both, I., Silvestri, C., Erdemir, T., Lickert, H., Walls, J.R., Henkelman, R.M., Rossant, J., Harvey, R.P., Attisano, L., and Wrana, J.L. (2004). Foxh1 is essential for development of the anterior heart field. Dev Cell *7*, 331-345.

70. Kirk, E.P., Sunde, M., Costa, M.W., Rankin, S.A., Wolstein, O., Castro, M.L., Butler, T.L., Hyun, C., Guo, G., Otway, R., et al. (2007). Mutations in cardiac T-box factor gene TBX20 are associated with diverse cardiac pathologies, including defects of septation and valvulogenesis and cardiomyopathy. Am J Hum Genet *81*, 280-291.

71. Pashmforoush, M., Lu, J.T., Chen, H., Amand, T.S., Kondo, R., Pradervand, S., Evans, S.M., Clark, B., Feramisco, J.R., Giles, W., et al. (2004). Nkx2-5 pathways and congenital heart disease; loss of ventricular myocyte lineage specification leads to progressive cardiomyopathy and complete heart block. Cell *117*, 373-386.

72. Loffredo, C.A. (2000). Epidemiology of cardiovascular malformations: prevalence and risk factors. Am J Med Genet *97*, 319-325.

73. Srivastava, D., and Olson, E.N. (2000). A genetic blueprint for cardiac development. Nature *407*, 221-226.

74. Armstrong, E.J., and Bischoff, J. (2004). Heart valve development: endothelial cell signaling and differentiation. Circulation research *95*, 459-470.

75. Tartaglia, M., Mehler, E.L., Goldberg, R., Zampino, G., Brunner, H.G., Kremer, H., van der Burgt, I., Crosby, A.H., Ion, A., Jeffery, S., et al. (2001). Mutations in PTPN11, encoding the protein tyrosine phosphatase SHP-2, cause Noonan syndrome. Nature genetics *29*, 465-468.

76. Li, L., Krantz, I.D., Deng, Y., Genin, A., Banta, A.B., Collins, C.C., Qi, M., Trask, B.J., Kuo, W.L., Cochran, J., et al. (1997). Alagille syndrome is caused by mutations in human Jagged1, which encodes a ligand for Notch1. Nature genetics *16*, 243-251.

77. Oda, T., Elkahloun, A.G., Pike, B.L., Okajima, K., Krantz, I.D., Genin, A., Piccoli, D.A., Meltzer, P.S., Spinner, N.B., Collins, F.S., et al. (1997). Mutations in the human Jagged1 gene are responsible for Alagille syndrome. Nature genetics *16*, 235-242.

78. Anderson, R.H., Webb, S., Brown, N.A., Lamers, W., and Moorman, A. (2003). Development of the heart: (2) Septation of the atriums and ventricles. Heart *89*, 949-958.

79. Markwald, R.R., Fitzharris, T.P., and Manasek, F.J. (1977). Structural development of endocardial cushions. Am J Anat *148*, 85-119.

80. Hinton, R.B., Jr., Lincoln, J., Deutsch, G.H., Osinska, H., Manning, P.B., Benson, D.W., and Yutzey, K.E. (2006). Extracellular matrix remodeling and organization in developing and diseased aortic valves. Circulation research *98*, 1431-1438.

81. Eisenberg, L.M., and Markwald, R.R. (1995). Molecular regulation of atrioventricular valvuloseptal morphogenesis. Circulation research *77*, 1-6.

82. Runyan, R.B., and Markwald, R.R. (1983). Invasion of mesenchyme into three-dimensional collagen gels: a regional and temporal analysis of interaction in embryonic heart tissue. Dev Biol *95*, 108-114.

83. Timmerman, L.A., Grego-Bessa, J., Raya, A., Bertran, E., Perez-Pomares, J.M., Diez, J., Aranda, S., Palomo, S., McCormick, F., Izpisua-Belmonte, J.C., et al. (2004). Notch promotes epithelial-mesenchymal transition during cardiac development and oncogenic transformation. Genes Dev *18*, 99-115.

84. Lyons, K.M., Pelton, R.W., and Hogan, B.L. (1990). Organogenesis and pattern formation in the mouse: RNA distribution patterns suggest a role for bone morphogenetic protein-2A (BMP-2A). Development *109*, 833-844.

85. Ma, L., Lu, M.F., Schwartz, R.J., and Martin, J.F. (2005). Bmp2 is essential for cardiac cushion epithelial-mesenchymal transition and myocardial patterning. Development *132*, 5601-5611.

86. Krug, E.L., Runyan, R.B., and Markwald, R.R. (1985). Protein extracts from early embryonic hearts initiate cardiac endothelial cytodifferentiation. Dev Biol *112*, 414-426.

87. Nakajima, Y., Yamagishi, T., Hokari, S., and Nakamura, H. (2000). Mechanisms involved in valvuloseptal endocardial cushion formation in early cardiogenesis: roles of transforming growth factor (TGF)-beta and bone morphogenetic protein (BMP). Anat Rec *258*, 119-127.

88. Sugi, Y., Yamamura, H., Okagawa, H., and Markwald, R.R. (2004). Bone morphogenetic protein-2 can mediate myocardial regulation of atrioventricular cushion mesenchymal cell formation in mice. Dev Biol *269*, 505-518.

89. Rivera-Feliciano, J., and Tabin, C.J. (2006). Bmp2 instructs cardiac progenitors to form the heart-valve-inducing field. Dev Biol *295*, 580-588.

90. Yamagishi, T., Nakajima, Y., Miyazono, K., and Nakamura, H. (1999). Bone morphogenetic protein-2 acts synergistically with transforming growth factor-beta3 during endothelial-mesenchymal transformation in the developing chick heart. J Cell Physiol *180*, 35-45.

91. Kim, R.Y., Robertson, E.J., and Solloway, M.J. (2001). Bmp6 and Bmp7 are required for cushion formation and septation in the developing mouse heart. Dev Biol *235*, 449-466.

92. Gaussin, V., Van de Putte, T., Mishina, Y., Hanks, M.C., Zwijsen, A., Huylebroeck, D., Behringer, R.R., and Schneider, M.D. (2002). Endocardial cushion and myocardial defects after cardiac myocyte-specific conditional deletion of the bone morphogenetic protein receptor ALK3. Proc Natl Acad Sci U S A *99*, 2878-2883.

93. Combs, M.D., and Yutzey, K.E. (2009). Heart valve development: regulatory networks in development and disease. Circulation research *105*, 408-421.

94. Romano, L.A., and Runyan, R.B. (2000). Slug is an essential target of TGFbeta2 signaling in the developing chicken heart. Dev Biol *223*, 91-102.

95. Liebner, S., Cattelino, A., Gallini, R., Rudini, N., Iurlaro, M., Piccolo, S., and Dejana, E. (2004). Beta-catenin is required for endothelial-mesenchymal transformation during heart cushion development in the mouse. J Cell Biol *166*, 359-367.

96. Hurlstone, A.F., Haramis, A.P., Wienholds, E., Begthel, H., Korving, J., Van Eeden, F., Cuppen, E., Zivkovic, D., Plasterk, R.H., and Clevers, H. (2003). The Wnt/beta-catenin pathway regulates cardiac valve formation. Nature *425*, 633-637.

97. Garg, V., Muth, A.N., Ransom, J.F., Schluterman, M.K., Barnes, R., King, I.N., Grossfeld, P.D., and Srivastava, D. (2005). Mutations in NOTCH1 cause aortic valve disease. Nature *437*, 270-274.

98. Krantz, I.D., Piccoli, D.A., and Spinner, N.B. (1999). Clinical and molecular genetics of Alagille syndrome. Curr Opin Pediatr *11*, 558-564.

99. Day, A.J., and Prestwich, G.D. (2002). Hyaluronan-binding proteins: tying up the giant. J Biol Chem *277*, 4585-4588.

100. Camenisch, T.D., Spicer, A.P., Brehm-Gibson, T., Biesterfeldt, J., Augustine, M.L., Calabro, A., Jr., Kubalak, S., Klewer, S.E., and McDonald, J.A. (2000). Disruption of hyaluronan synthase-2 abrogates normal cardiac morphogenesis and hyaluronan-mediated transformation of epithelium to mesenchyme. J Clin Invest *106*, 349-360.

101. Camenisch, T.D., Schroeder, J.A., Bradley, J., Klewer, S.E., and McDonald, J.A. (2002). Heart-valve mesenchyme formation is dependent on hyaluronan-augmented activation of ErbB2-ErbB3 receptors. Nat Med *8*, 850-855.

102. Erickson, S.L., O'Shea, K.S., Ghaboosi, N., Loverro, L., Frantz, G., Bauer, M., Lu, L.H., and Moore, M.W. (1997). ErbB3 is required for normal cerebellar and cardiac development: a comparison with ErbB2-and heregulin-deficient mice. Development *124*, 4999-5011.

103. Stainier, D.Y., Fouquet, B., Chen, J.N., Warren, K.S., Weinstein, B.M., Meiler, S.E., Mohideen, M.A., Neuhauss, S.C., Solnica-Krezel, L., Schier, A.F., et al. (1996). Mutations affecting the formation and function of the cardiovascular system in the zebrafish embryo. Development *123*, 285-292.

104. Walsh, E.C., and Stainier, D.Y. (2001). UDP-glucose dehydrogenase required for cardiac valve formation in zebrafish. Science *293*, 1670-1673.

105. Jiao, K., Kulessa, H., Tompkins, K., Zhou, Y., Batts, L., Baldwin, H.S., and Hogan, B.L. (2003). An essential role of Bmp4 in the atrioventricular septation of the mouse heart. Genes Dev *17*, 2362-2367.

106. McCulley, D.J., Kang, J.O., Martin, J.F., and Black, B.L. (2008). BMP4 is required in the anterior heart field and its derivatives for endocardial cushion remodeling, outflow tract septation, and semilunar valve development. Dev Dyn *237*, 3200-3209.

107. Delot, E.C., Bahamonde, M.E., Zhao, M., and Lyons, K.M. (2003). BMP signaling is required for septation of the outflow tract of the mammalian heart. Development *130*, 209-220.

108. Galvin, K.M., Donovan, M.J., Lynch, C.A., Meyer, R.I., Paul, R.J., Lorenz, J.N., Fairchild-Huntress, V., Dixon, K.L., Dunmore, J.H., Gimbrone, M.A., Jr., et al. (2000). A role for smad6 in development and homeostasis of the cardiovascular system. Nature genetics *24*, 171-174.

109. Takase, M., Imamura, T., Sampath, T.K., Takeda, K., Ichijo, H., Miyazono, K., and Kawabata, M. (1998). Induction of Smad6 mRNA by bone morphogenetic proteins. Biochem Biophys Res Commun *244*, 26-29.

110. Yarden, Y., and Sliwkowski, M.X. (2001). Untangling the ErbB signalling network. Nat Rev Mol Cell Biol *2*, 127-137.

111. Chen, B., Bronson, R.T., Klaman, L.D., Hampton, T.G., Wang, J.F., Green, P.J., Magnuson, T., Douglas, P.S., Morgan, J.P., and Neel, B.G. (2000). Mice mutant for Egfr and Shp2 have defective cardiac semilunar valvulogenesis. Nature genetics *24*, 296-299.

112. Krenz, M., Gulick, J., Osinska, H.E., Colbert, M.C., Molkentin, J.D., and Robbins, J. (2008). Role of ERK1/2 signaling in congenital valve malformations in Noonan syndrome. Proc Natl Acad Sci U S A *105*, 18930-18935.

113. Jackson, L.F., Qiu, T.H., Sunnarborg, S.W., Chang, A., Zhang, C., Patterson, C., and Lee, D.C. (2003). Defective valvulogenesis in HB-EGF and TACE-null mice is associated with aberrant BMP signaling. Embo J *22*, 2704-2716.

114. Ferrara, N., Gerber, H.P., and LeCouter, J. (2003). The biology of VEGF and its receptors. Nat Med *9*, 669-676.

115. Dor, Y., Camenisch, T.D., Itin, A., Fishman, G.I., McDonald, J.A., Carmeliet, P., and Keshet, E. (2001). A novel role for VEGF in endocardial cushion formation and its potential contribution to congenital heart defects. Development *128*, 1531-1538.

116. Miquerol, L., Langille, B.L., and Nagy, A. (2000). Embryonic development is disrupted by modest increases in vascular endothelial growth factor gene expression. Development *127*, 3941-3946.

117. Lee, Y.M., Cope, J.J., Ackermann, G.E., Goishi, K., Armstrong, E.J., Paw, B.H., and Bischoff, J. (2006). Vascular endothelial growth factor receptor signaling is required for cardiac valve formation in zebrafish. Dev Dyn *235*, 29-37.

118. de la Pompa, J.L., Timmerman, L.A., Takimoto, H., Yoshida, H., Elia, A.J., Samper, E., Potter, J., Wakeham, A., Marengere, L., Langille, B.L., et al. (1998). Role of the NF-ATc transcription factor in morphogenesis of cardiac valves and septum. Nature *392*, 182-186.

119. Ranger, A.M., Grusby, M.J., Hodge, M.R., Gravallese, E.M., de la Brousse, F.C., Hoey, T., Mickanin, C., Baldwin, H.S., and Glimcher, L.H. (1998). The transcription factor NF-ATc is essential for cardiac valve formation. Nature *392*, 186-190.

120. Johnson, E.N., Lee, Y.M., Sander, T.L., Rabkin, E., Schoen, F.J., Kaushal, S., and Bischoff, J. (2003). NFATc1 mediates vascular endothelial growth factor-induced proliferation of human pulmonary valve endothelial cells. J Biol Chem *278*, 1686-1692.

121. Libert, F., Parmentier, M., Lefort, A., Dumont, J.E., and Vassart, G. (1990). Complete nucleotide sequence of a putative G protein coupled receptor: RDC1. Nucleic Acids Res *18*, 1917.

122. Libert, F., Passage, E., Parmentier, M., Simons, M.J., Vassart, G., and Mattei, M.G. (1991). Chromosomal mapping of A1 and A2 adenosine receptors, VIP receptor, and a new subtype of serotonin receptor. Genomics *11*, 225-227.

123. Cook, J.S., Wolsing, D.H., Lameh, J., Olson, C.A., Correa, P.E., Sadee, W., Blumenthal, E.M., and Rosenbaum, J.S. (1992). Characterization of the RDC1 gene which encodes the canine homolog of a proposed human VIP receptor. Expression does not correlate with an increase in VIP binding sites. FEBS Lett *300*, 149-152.

124. Nagata, S., Ishihara, T., Robberecht, P., Libert, F., Parmentier, M., Christophe, J., and Vassart, G. (1992). RDC1 may not be VIP receptor. Trends Pharmacol Sci *13*, 102-103.

125. Heesen, M., Berman, M.A., Charest, A., Housman, D., Gerard, C., and Dorf, M.E. (1998). Cloning and chromosomal mapping of an orphan chemokine receptor: mouse RDC1. Immunogenetics *47*, 364-370.

126. Fredriksson, R., Lagerstrom, M.C., Lundin, L.G., and Schioth, H.B. (2003). The G-protein-coupled receptors in the human genome form five main families. Phylogenetic analysis, paralogon groups, and fingerprints. Mol Pharmacol *63*, 1256-1272.

127. Joost, P., and Methner, A. (2002). Phylogenetic analysis of 277 human G-protein-coupled receptors as a tool for the prediction of orphan receptor ligands. Genome Biol *3*, RESEARCH0063.

128. Shimizu, N., Soda, Y., Kanbe, K., Liu, H.Y., Mukai, R., Kitamura, T., and Hoshino, H. (2000). A putative G protein-coupled receptor, RDC1, is a novel coreceptor for human and simian immunodeficiency viruses. J Virol *74*, 619-626.

129. Thelen, M., and Thelen, S. (2008). CXCR7, CXCR4 and CXCL12: an eccentric trio? J Neuroimmunol *198*, 9-13.

130. Balabanian, K., Lagane, B., Infantino, S., Chow, K.Y., Harriague, J., Moepps, B., Arenzana-Seisdedos, F., Thelen, M., and Bachelerie, F. (2005). The chemokine

SDF-1/CXCL12 binds to and signals through the orphan receptor RDC1 in T lymphocytes. J Biol Chem *280*, 35760-35766.

131. Burns, J.M., Summers, B.C., Wang, Y., Melikian, A., Berahovich, R., Miao, Z., Penfold, M.E., Sunshine, M.J., Littman, D.R., Kuo, C.J., et al. (2006). A novel chemokine receptor for SDF-1 and I-TAC involved in cell survival, cell adhesion, and tumor development. J Exp Med *203*, 2201-2213.

132. Nagasawa, T., Hirota, S., Tachibana, K., Takakura, N., Nishikawa, S., Kitamura, Y., Yoshida, N., Kikutani, H., and Kishimoto, T. (1996). Defects of B-cell lymphopoiesis and bone-marrow myelopoiesis in mice lacking the CXC chemokine PBSF/SDF-1. Nature *382*, 635-638.

133. Ma, Q., Jones, D., Borghesani, P.R., Segal, R.A., Nagasawa, T., Kishimoto, T., Bronson, R.T., and Springer, T.A. (1998). Impaired B-lymphopoiesis, myelopoiesis, and derailed cerebellar neuron migration in CXCR4- and SDF-1-deficient mice. Proc Natl Acad Sci U S A *95*, 9448-9453.

134. Zou, Y.R., Kottmann, A.H., Kuroda, M., Taniuchi, I., and Littman, D.R. (1998). Function of the chemokine receptor CXCR4 in haematopoiesis and in cerebellar development. Nature *393*, 595-599.

135. Tachibana, K., Hirota, S., Iizasa, H., Yoshida, H., Kawabata, K., Kataoka, Y., Kitamura, Y., Matsushima, K., Yoshida, N., Nishikawa, S., et al. (1998). The chemokine receptor CXCR4 is essential for vascularization of the gastrointestinal tract. Nature *393*, 591-594.

136. Hartmann, T.N., Grabovsky, V., Pasvolsky, R., Shulman, Z., Buss, E.C., Spiegel, A., Nagler, A., Lapidot, T., Thelen, M., and Alon, R. (2008). A crosstalk between intracellular CXCR7 and CXCR4 involved in rapid CXCL12-triggered integrin activation but not in chemokine-triggered motility of human T lymphocytes and CD34+ cells. J Leukoc Biol *84*, 1130-1140.

137. Boldajipour, B., Mahabaleshwar, H., Kardash, E., Reichman-Fried, M., Blaser, H., Minina, S., Wilson, D., Xu, Q., and Raz, E. (2008). Control of chemokine-guided cell migration by ligand sequestration. Cell *132*, 463-473.

138. Proost, P., Mortier, A., Loos, T., Vandercappellen, J., Gouwy, M., Ronsse, I., Schutyser, E., Put, W., Parmentier, M., Struyf, S., et al. (2007). Proteolytic processing of CXCL11 by CD13/aminopeptidase N impairs CXCR3 and CXCR7 binding and signaling and reduces lymphocyte and endothelial cell migration. Blood *110*, 37-44.

139. Dambly-Chaudiere, C., Cubedo, N., and Ghysen, A. (2007). Control of cell migration in the development of the posterior lateral line: antagonistic

interactions between the chemokine receptors CXCR4 and CXCR7/RDC1. BMC Dev Biol *7*, 23.

140. Infantino, S., Moepps, B., and Thelen, M. (2006). Expression and regulation of the orphan receptor RDC1 and its putative ligand in human dendritic and B cells. J Immunol *176*, 2197-2207.

141. Mazzinghi, B., Ronconi, E., Lazzeri, E., Sagrinati, C., Ballerini, L., Angelotti, M.L., Parente, E., Mancina, R., Netti, G.S., Becherucci, F., et al. (2008). Essential but differential role for CXCR4 and CXCR7 in the therapeutic homing of human renal progenitor cells. J Exp Med *205*, 479-490.

142. Thelen, M. (2001). Dancing to the tune of chemokines. Nat Immunol *2*, 129-134.

143. Raggo, C., Ruhl, R., McAllister, S., Koon, H., Dezube, B.J., Fruh, K., and Moses, A.V. (2005). Novel cellular genes essential for transformation of endothelial cells by Kaposi's sarcoma-associated herpesvirus. Cancer Res *65*, 5084-5095.

144. Goldmann, T., Dromann, D., Radtke, J., Marwitz, S., Lang, D.S., Schultz, H., and Vollmer, E. (2008). CXCR7 transcription in human non-small cell lung cancer and tumor-free lung tissues; possible regulation upon chemotherapy. Virchows Arch *452*, 347-348.

145. Schutyser, E., Su, Y., Yu, Y., Gouwy, M., Zaja-Milatovic, S., Van Damme, J., and Richmond, A. (2007). Hypoxia enhances CXCR4 expression in human microvascular endothelial cells and human melanoma cells. Eur Cytokine Netw *18*, 59-70.

146. Wang, J., Shiozawa, Y., Wang, Y., Jung, Y., Pienta, K.J., Mehra, R., Loberg, R., and Taichman, R.S. (2008). The role of CXCR7/RDC1 as a chemokine receptor for CXCL12/SDF-1 in prostate cancer. J Biol Chem *283*, 4283-4294.

147. Miao, Z., Luker, K.E., Summers, B.C., Berahovich, R., Bhojani, M.S., Rehemtulla, A., Kleer, C.G., Essner, J.J., Nasevicius, A., Luker, G.D., et al. (2007). CXCR7 (RDC1) promotes breast and lung tumor growth in vivo and is expressed on tumor-associated vasculature. Proc Natl Acad Sci U S A *104*, 15735-15740.

148. Madden, S.L., Cook, B.P., Nacht, M., Weber, W.D., Callahan, M.R., Jiang, Y., Dufault, M.R., Zhang, X., Zhang, W., Walter-Yohrling, J., et al. (2004). Vascular gene expression in nonneoplastic and malignant brain. Am J Pathol *165*, 601-608.

149. Zabel, B.A., Wang, Y., Lewen, S., Berahovich, R.D., Penfold, M.E., Zhang, P., Powers, J., Summers, B.C., Miao, Z., Zhao, B., et al. (2009). Elucidation of

CXCR7-Mediated Signaling Events and Inhibition of CXCR4-Mediated Tumor Cell Transendothelial Migration by CXCR7 Ligands. J Immunol.

150. Valentin, G., Haas, P., and Gilmour, D. (2007). The chemokine SDF1a coordinates tissue migration through the spatially restricted activation of Cxcr7 and Cxcr4b. Curr Biol *17*, 1026-1031.

151. Kalatskaya, I., Berchiche, Y.A., Gravel, S., Limberg, B.J., Rosenbaum, J.S., and Heveker, N. (2009). AMD3100 is a CXCR7 ligand with allosteric agonist properties. Mol Pharmacol *75*, 1240-1247.

152. Sierro, F., Biben, C., Martinez-Munoz, L., Mellado, M., Ransohoff, R.M., Li, M., Woehl, B., Leung, H., Groom, J., Batten, M., et al. (2007). Disrupted cardiac development but normal hematopoiesis in mice deficient in the second CXCL12/SDF-1 receptor, CXCR7. Proc Natl Acad Sci U S A *104*, 14759-14764.

153. Levoye, A., Balabanian, K., Baleux, F., Bachelerie, F., and Lagane, B. (2009). CXCR7 heterodimerizes with CXCR4 and regulates CXCL12-mediated G protein signaling. Blood *113*, 6085-6093.

154. Comerford, I., and Nibbs, R.J. (2005). Post-translational control of chemokines: a role for decoy receptors? Immunology letters *96*, 163-174.

155. Lamers, W.H., and Moorman, A.F. (2002). Cardiac septation: a late contribution of the embryonic primary myocardium to heart morphogenesis. Circulation research *91*, 93-103.

156. Hutson, M.R., and Kirby, M.L. (2007). Model systems for the study of heart development and disease. Cardiac neural crest and conotruncal malformations. Seminars in cell & developmental biology *18*, 101-110.

157. Nishibatake, M., Kirby, M.L., and Van Mierop, L.H. (1987). Pathogenesis of persistent truncus arteriosus and dextroposed aorta in the chick embryo after neural crest ablation. Circulation *75*, 255-264.

158. Yelbuz, T.M., Waldo, K.L., Kumiski, D.H., Stadt, H.A., Wolfe, R.R., Leatherbury, L., and Kirby, M.L. (2002). Shortened outflow tract leads to altered cardiac looping after neural crest ablation. Circulation *106*, 504-510.

159. Steventon, B., Carmona-Fontaine, C., and Mayor, R. (2005). Genetic network during neural crest induction: from cell specification to cell survival. Seminars in cell & developmental biology *16*, 647-654.

160. Schwenk, F., Baron, U., and Rajewsky, K. (1995). A cre-transgenic mouse strain for the ubiquitous deletion of loxP-flanked gene segments including deletion in germ cells. Nucleic Acids Res *23*, 5080-5081.

161. Frey, N., Katus, H.A., Olson, E.N., and Hill, J.A. (2004). Hypertrophy of the heart: a new therapeutic target? Circulation *109*, 1580-1589.

162. Backs, J., and Olson, E.N. (2006). Control of cardiac growth by histone acetylation/deacetylation. Circulation research *98*, 15-24.

163. Jessup, M., and Brozena, S. (2003). Heart failure. N Engl J Med *348*, 2007-2018.

164. Rajamannan, N.M., Gersh, B., and Bonow, R.O. (2003). Calcific aortic stenosis: from bench to the bedside--emerging clinical and cellular concepts. Heart *89*, 801-805.

165. Kretzschmar, M., Doody, J., and Massague, J. (1997). Opposing BMP and EGF signalling pathways converge on the TGF-beta family mediator Smad1. Nature *389*, 618-622.

166. Lo, R.S., Wotton, D., and Massague, J. (2001). Epidermal growth factor signaling via Ras controls the Smad transcriptional co-repressor TGIF. The EMBO journal *20*, 128-136.

167. Nonaka, K., Shum, L., Takahashi, I., Takahashi, K., Ikura, T., Dashner, R., Nuckolls, G.H., and Slavkin, H.C. (1999). Convergence of the BMP and EGF signaling pathways on Smad1 in the regulation of chondrogenesis. The International journal of developmental biology *43*, 795-807.

168. Delot, E.C. (2003). Control of endocardial cushion and cardiac valve maturation by BMP signaling pathways. Molecular genetics and metabolism *80*, 27-35.

169. Gerrits, H., van Ingen Schenau, D.S., Bakker, N.E., van Disseldorp, A.J., Strik, A., Hermens, L.S., Koenen, T.B., Krajnc-Franken, M.A., and Gossen, J.A. (2008). Early postnatal lethality and cardiovascular defects in CXCR7-deficient mice. Genesis *46*, 235-245.

170. Cubedo, N., Cerdan, E., Sapede, D., and Rossel, M. (2009). CXCR4 and CXCR7 cooperate during tangential migration of facial motoneurons. Mol Cell Neurosci *40*, 474-484.

171. Jones, S.W., Brockbank, S.M., Mobbs, M.L., Le Good, N.J., Soma-Haddrick, S., Heuze, A.J., Langham, C.J., Timms, D., Newham, P., and Needham, M.R. (2006). The orphan G-protein coupled receptor RDC1: evidence for a role in chondrocyte hypertrophy and articular cartilage matrix turnover. Osteoarthritis and cartilage / OARS, Osteoarthritis Research Society *14*, 597-608.

172. Meyers, E.N., Lewandoski, M., and Martin, G.R. (1998). An Fgf8 mutant allelic series generated by Cre- and Flp-mediated recombination. Nature genetics *18*, 136-141.